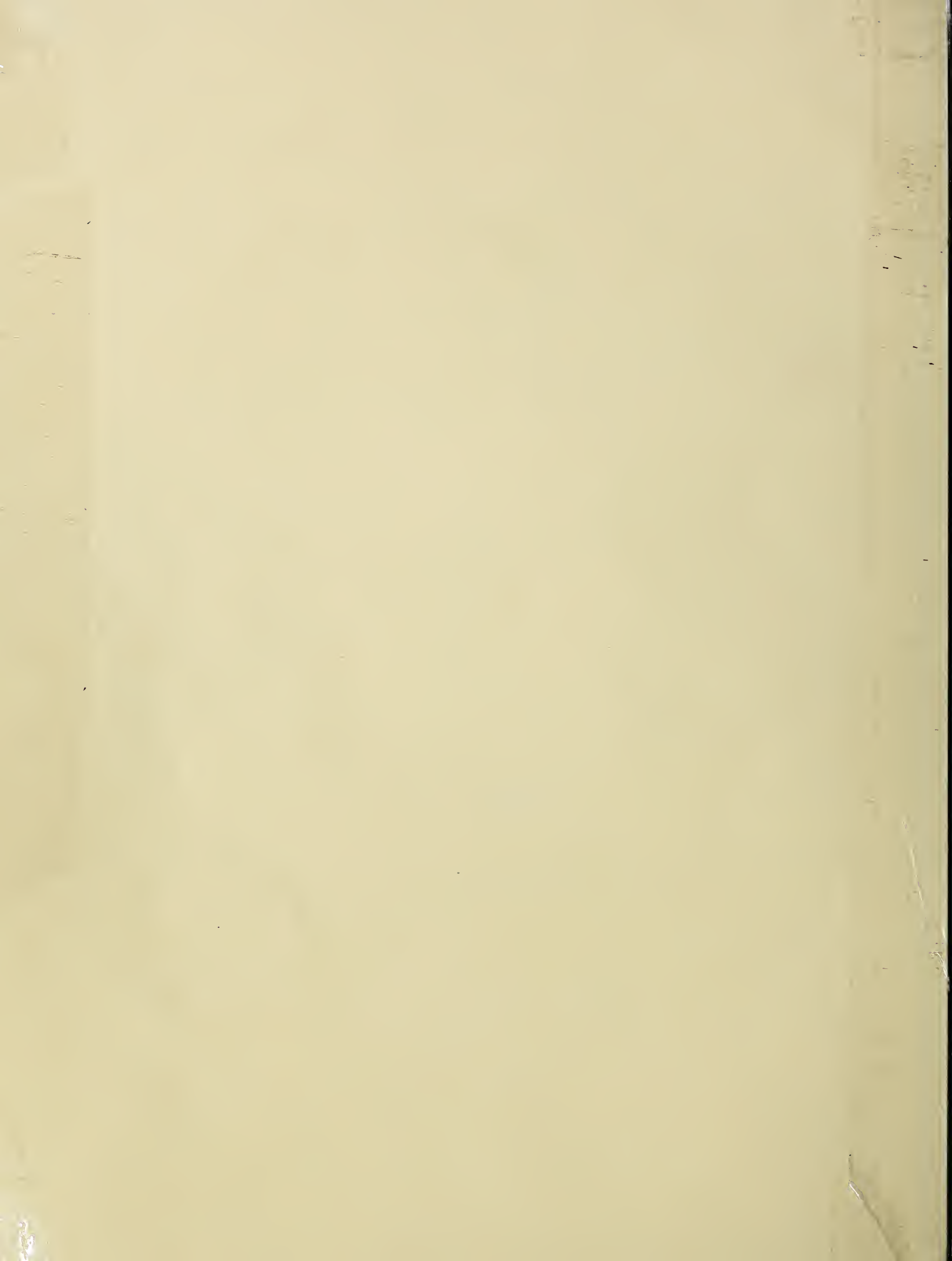


## **Historic, Archive Document**

Do not assume content reflects current scientific knowledge, policies, or practices.



Reserve

aTA423

.2

.P76

1989

**United States  
Department of  
Agriculture**



**National Agricultural Library**

AUG 17 1995

Document No: IRG/WP/ 1391

CATALOGING PREP.

THE INTERNATIONAL RESEARCH GROUP ON WOOD PRESERVATION

Working Group I a

Biological Problems (Flora)

PROPOSED MODEL FOR THE PENETRATION AND DECAY OF WOOD BY  
THE HYPHAL SHEATH OF THE BROWN-ROT FUNGUS POSTIA PLACENTA.

by

F. Green, M. J. Larsen, L. L. Murmanis, and T. L. Highley

U.S. Department of Agriculture, Forest Service  
Forest Products Laboratory  
One Gifford Pinchot Drive  
Madison, Wisconsin, USA 53705-2398

Paper prepared for Twentieth Annual Meeting

Lappeenranta, Finland  
21-26, May 1989

IRG Secretariat  
Drottning Distinas vag 47 C  
S-114 28 Stockholm  
Sweden

4 March 1989





PROPOSED MODEL FOR THE PENETRATION AND DECAY OF WOOD  
BY THE HYPHAL SHEATH OF THE BROWN-ROT FUNGUS POSTIA PLACENTA.

By

Green, F., M.J. Larsen, L.L. Murmanis, and T.L. Highley  
U.S. Department of Agriculture, Forest Service  
Forest Products Laboratory<sup>1</sup>, Madison, WI, USA 53705-2398

SUMMARY

Scanning electron microscopy (SEM) of Pinus sp. decayed by the brown-rot fungus Postia placenta confirmed the existence of extracellular membranous structures previously described by transmission electron microscopy (TEM). These structures appear to be an integral part of the hyphal sheath and assume a variety of forms including lamellar sheets, fibrils, and vesicles. These structures were observed (a) on the surface of hyphae, (b) extending from hyphae onto the wood surface and covering the  $S_3$  layer, (c) embedded in the hyphal sheath and, (d) penetrating into the wood cell wall layers from  $S_3$ - $S_3$ .

We conclude that penetration of the wood cell wall by the complex, multistructured hyphal sheath facilitates the decay process in an orderly and linear progression. The directionality of the decay process appears to alter the fiber orientation of individual wood cell wall layers. This model offers an alternative hypothesis to simple diffusion of wood degrading agents during wood decay by P. placenta.

Keywords: Brown-rot, wood decay, hyphal sheath, extracellular membranous structures, wood anatomy, electron microscopy (SEM).

INTRODUCTION

Our current understanding of the ultrastructural micromorphology of wood-fungus interactions during wood decay, has been derived in large part from transmission electron micrographs (TEM) (12, 13, 19, 30, 33). Thus, observations have been restricted to a thin two-dimensional plane providing salient but limited information on the modifications of wood during the decay process. Questions specifically addressing enzyme penetration and decay progression have not been satisfactorily resolved by TEM (8, 30, 31, 32).

There is an apparent void in the literature between early observations on the decay fungi in wood by SEM and the present (4, 11, 14, 20, 21, 27). Many of the earlier papers present low magnification SEM micrographs limited to

---

<sup>1</sup>The Forest Products Laboratory is maintained in cooperation with the University of Wisconsin. This article as written and prepared by U.S. Government employees on official time, and it is therefore in the public domain and not subject to copyright.

surface phenomena of the  $S_3$ . The current availability of high resolution scanning electron microscopes, concurrent with improvements in creative methodology of SEM specimen preparation provides an additional correlate to TEM for ultrastructural studies. Application of SEM technology should confirm fungal and wood structures during decay previously detailed by TEM.

In a series of provocative publications Foisner et al. (12, 13) and Messner et al. (25, 26, 27) described in detail for the first time, using transmission electron microscopy, extracellular membranous structures (sheath of brown- and white-rot basidiomycetes, and suggested a possible role for these structures in wood decay.

Extracellular layers (hyphal sheath) enveloping vegetative hyphae of fungi are a common morphological feature (2, 29). Hyphal sheaths are postulated to provide several functions for living hyphae; e.g., (a) attachment to solid substrates, (b) a nutrient reserve, (c) reduce dessication and nutrient loss, (d) provide protection against toxic chemicals, (e) facilitate wood degradation by storing or concentrating wood degrading agents (f) maintain a favorable moisture/pH environment for enzyme activity, and (g) conditioning the substrate prior to enzyme action (17).

The results presented in this communication confirm by SEM the existence of extracellular membranous structures of the brown-rot fungus P. placenta, and penetration of wood cell-wall layers by these structures. These results also provide a supplemental mechanism to account for distribution of wood decay agents during brown-rot decay.

#### MATERIALS AND METHODS

Wood blocks (8 x 8 x 4 mm) of southern yellow pine (Pinus sp.) were decayed by the brown-rot fungus Postia placenta (Fr.) M. Lars. et Lomb. (isolate no. MAD-698) using the ASTM soil-block procedure (1). At intervals during the 2-13 week decay period, selected blocks were removed and rapidly quenched in precooled (30 psi, -210C) liquid nitrogen ( $N_2$ ) without chemical fixation. After 15 minutes blocks were transferred to a precooled cryovessel and lyophilized overnight (ca. 12 hours). Blocks prepared in this manner were then split longitudinally with a razor blade to expose the radial face, and then coated with gold (Au) on a Balzer's sputter-coater for 22 sec. resulting in an Au-layer ca. 65-70 Å thick. Additional blocks were fixed by exposure to vapors of osmium tetroxide (1%) in an environmental hood, air dried, and gold coated as above. Specimens were observed with the aid of a Hitachi S-530 scanning electron microscope at an accelerating voltage of 20-25 Kv. Working distances were ca. 5-10 mm.



## RESULTS

Degradation of southern yellow pine (*Pinus* sp.) by the brown-rot fungus *Postia placenta* is shown in figures 1-21. Figures 1 and 2 illustrate fungal hyphae in close proximity to the longitudinally fractured faces of the tracheid cell wall. Extracellular hyphal structures extending from the hyphal cell wall can be seen attached to the modified  $S_3$  of the cell wall, with decay pockets visible in the  $S_2$  layer (Fig. 2).

The  $S_3$  surface layer of nearly all tracheids observed in this study was covered by sheath matrix, thus obliterating the underlying wood fiber structure (Figs. 3-4). Although some tracheids examined contained more than one hypha, usually only a single hypha per tracheid appeared sufficient to mask the  $S_3$  surface with hyphal sheath and branched mycofibrils.

As decay progresses, linear penetration by mycofibrils across the  $S_3$  and into the  $S_2$  is observed extending from areas covered by hyphae and extracellular hyphal sheath, especially in close proximity to hyphae and hyphal sheath structures (Figs. 4-5). The mycofibrillar penetrations into cell walls resemble the structures of the modified  $S_3$  and penetrate radially from  $S_3$  to opposing  $S_3$  of adjacent tracheid walls. Prior to tangential penetration by mycofibrils into the  $S_2$ , preferential hydrolysis of the  $S_1$ - $S_2$  interface zone (z) of the wood cell wall was observed (Figs. 5-6). Microfibrils, similar in size to mycofibrils, are visible within this decay zone.

Extracellular hyphal structures are variable in size and configuration. Figures 7 and 8 illustrate branched, fused and vesicular manifestations of the hyphal sheath. Figure 9 demonstrates mycofibrils (approx. 50 nm in diam.) on a "hairy" hypha in contact with the wood cell surface. Hyphal sheath is also observed as a smooth bilayer overlaying the mycofibrils which arise from the fungal cell wall layer underneath the sheath (Fig. 10). Both sheath and fungal cell wall-associated mycofibrils extend onto the surface of the  $S_3$  and are shown fusing into a uniform and ubiquitous structure (Figs. 11-12).

Mycofibrillar structures are shown penetrating the modified  $S_3$  and  $S_2$  radially. The apparent orientation of the  $S_3$  layer now follows the radial penetration of the sheath mycofibrils. The radial orientation continues through the compound middle lamellae into the opposing cell wall (Figs. 13-15). Decay pockets in the radial plane also reveal mycofibrillar orientation to  $S_1$ - $S_2$  interface. The preferential hydrolysis of the  $S_1$ - $S_2$  interface (z) visible on the oblique surface (os) is obscured by mycofibrils or sheath on the longitudinal surface (ls) (Fig. 15). A membranous remnant, apparently bilayered, is visible (Fig. 15). Penetration of the  $S_2$  is evidenced by membranous and fibrillar sheath elements which extend from the  $S_3$  (Fig. 16). Mycofibrils and branched decay channels within the  $S_2$  and bridging the wood cell wall are evident in Figure 17. Fibrous sheath is visible within the tracheid lumen and continues linearly through the  $S_2$  layer of the opposing wood cell wall (Fig. 18). Additional representations of the extracellular membranous structures (m) are shown in apposition to modified  $S_3$  of the wood cell wall (Figs. 19, 20 and 21).

## DISCUSSION

Extracellular membranous and fibrillar structures were visualized by SEM extending from the hyphal cell wall and penetrating wood cell wall layers. These hyphal sheath structures provide an alternative model to account for



transport of wood degrading agents during decay progression. This model also provides a means for the uptake and transport of nutrients to the fungal protoplasts. The primary barrier to the existing simple diffusion model to explain the movement of wood decay enzymes has been the apparent lack of appropriately sized pores in cell wall layers required to permit diffusion of enzymes of the 30-60 kD range (15, 23, 24, 33, 34) even after decay has been initiated. Therefore, a low molecular weight, non-enzymatic system was postulated (23). The sheath may be necessary to predispose the cell wall layers, especially the modification of the  $S_3$ , as a prerequisite for penetration of decay enzymes. Furthermore, decay pores and channels may be progressively obstructed by sheath structures during decay, thus blocking simple diffusion.

Many of the underlying concepts and structures supporting this proposed model of penetration of decay agents by hyphal sheath components already exist in the literature. Numerous authors have suggested a role in fungus-host interactions for penetration hyphae, appressoria, haustoria, needle-like infection hyphae, and microhyphae (2, 10, 16, 24, 35). In a review of wood decay, Liese (24) illustrated "mycofibrils" of Chaetomium globosum Kunze, and suggested a role for these structures in penetration and decay. We concur with the use of the term 'mycofibril' to designate the structure observed here. We also propose consideration of the analogous term 'mycovesicle' to designate membranous vesicles exterior to the hyphal plasmalemma. Foisner et al. (12, 13) and Messner et al. (25, 26, 27) described hyphal cell wall systems and tripartite extracellular membranous structures of brown- and white-rot fungi. We conclude that the structures reported here from SEM are essentially the same as those reported in their studies. From TEM it is known that the hyphal sheath extends some distance away from the hyphae (12, 18, 25, 26, 29, 30), and is confirmed here by SEM. Wood decay, especially brown-rot, occurs in a ubiquitous fashion in the wood cell wall at great distances from the hyphae (4, 17, 18). Apparently, the small structures observed extending into the wood cell wall are difficult to resolve in TEM, possibly due to chemical modification during specimen preparation, elution or their inherent low electron density (electron lucent) in wood (2). Low molecular weight polysaccharides, such as water soluble  $\beta$ -1,3 (1,6) glucans, are known to be components of the hyphal sheath (17).

It is our understanding from TEM and SEM that mycofibrils and mycovesicles are modifications of the hyphal plasmalemma, similar to lomasomes (2), which arise in the periplasmic space of the hyphal cell (unpublished results). We propose that the fundamental unit of the extracellular hyphal sheath is the mycovesicle that can self-assemble within the fungal cell wall and coalesce to form a fluid and dynamic assemblage of extracellular structures (13). In concert with this perspective, we have observed that mycovesicles and mycofibrils appear to coalesce into lamellar sheets and differentiate into mycovesicles and mycofibrils during penetration of the wood cell wall. Sheath membranes, therefore, are probably "self-assembled" from large numbers of mycovesicles and mycofibrils (13). Foisner et al. (13) further characterized tripartite extracellular membranes biochemically as containing carbohydrate, lipid, and protein but without phospholipid. They concluded that these membranes are functionally different from plasma membranes. Bracker (3), reporting on Gilbertella, provided convincing evidence for the ability of biomembranes to undergo numerous morphological transformations, e.g., "vesicles, tubes, or sheets." We view the intracellular representations of Bracker's membranes as analogous to the extracellular hyphal sheath structures described here.



Inherent in the wood decay process is an intimate relationship between the underlying physical and biochemical structure of the wood cell wall and degradation by decay agents of Postia placenta. In this SEM study, the microfibrillar structure of decayed wood is modified by sheath structures. The estimated hemicellulose content of the  $S_3$ ,  $S_2$  matrix,  $S_1$ , CML and cell corners parallels sites of initial attack by P. placenta (9, 18, 31). Lignin is not an obvious chemical barrier to brown-rot decay by P. placenta, despite the apparent absence of lignin-specific enzymes that are formed in white rot fungi (e.g. Phanerochaete chrysosporium Burds. in Burds. et Eslyn). Brown-rot fungi have been reported to demethylate lignin resulting in an accumulation of polymeric degradation products (22). All cell wall layers are penetrated with rapid removal of hemicellulose (6, 17). Hemicellulose content is high at the  $S_1$ - $S_2$  and  $S_2$ - $S_3$  interfaces (32), predisposing the cell wall to preferential hydrolysis at these interfaces. A similar pattern of selective decay has been reported for Schizophyllum commune Fr. on Pinus sylvestris L. (7). However, in our study the rapid hydrolysis at the  $S_1$ - $S_2$  interface may also be explained by direct penetration by decay agents from transverse surfaces of colonized wood blocks.

Decay of the compound middle lamella and penetration of hyphae into cell wall corners has been previously reported using TEM (18). The mechanisms by which P. placenta modify or oxidize lignin during removal of hemicellulose and cellulose remains obscure (18, 22). Subsequent reagglomeration or precipitation of modified lignin residues appears similar to residues which remain following enzyme hydrolysis and steam explosion (9,10). Fracture faces of decayed and dehydrated wood blocks are most likely to occur in the weakest planes. Thus, selective decay and penetration of existing wood cell-wall structure by P. placenta apparently reveals underlying physical or chemical structure not evident in undecayed control blocks (unpublished results). Progressive penetration of Pinus wood by P. placenta appears linear and perpendicular to the tracheid cell wall. This directionality of decay penetration has been previously documented by TEM (18, 32). Some anatomical features of wood structure revealed by P. placenta appear similar to those observed in Douglas-fir following removal of cellulose and hemicellulose by hydrofluoric acid (5).

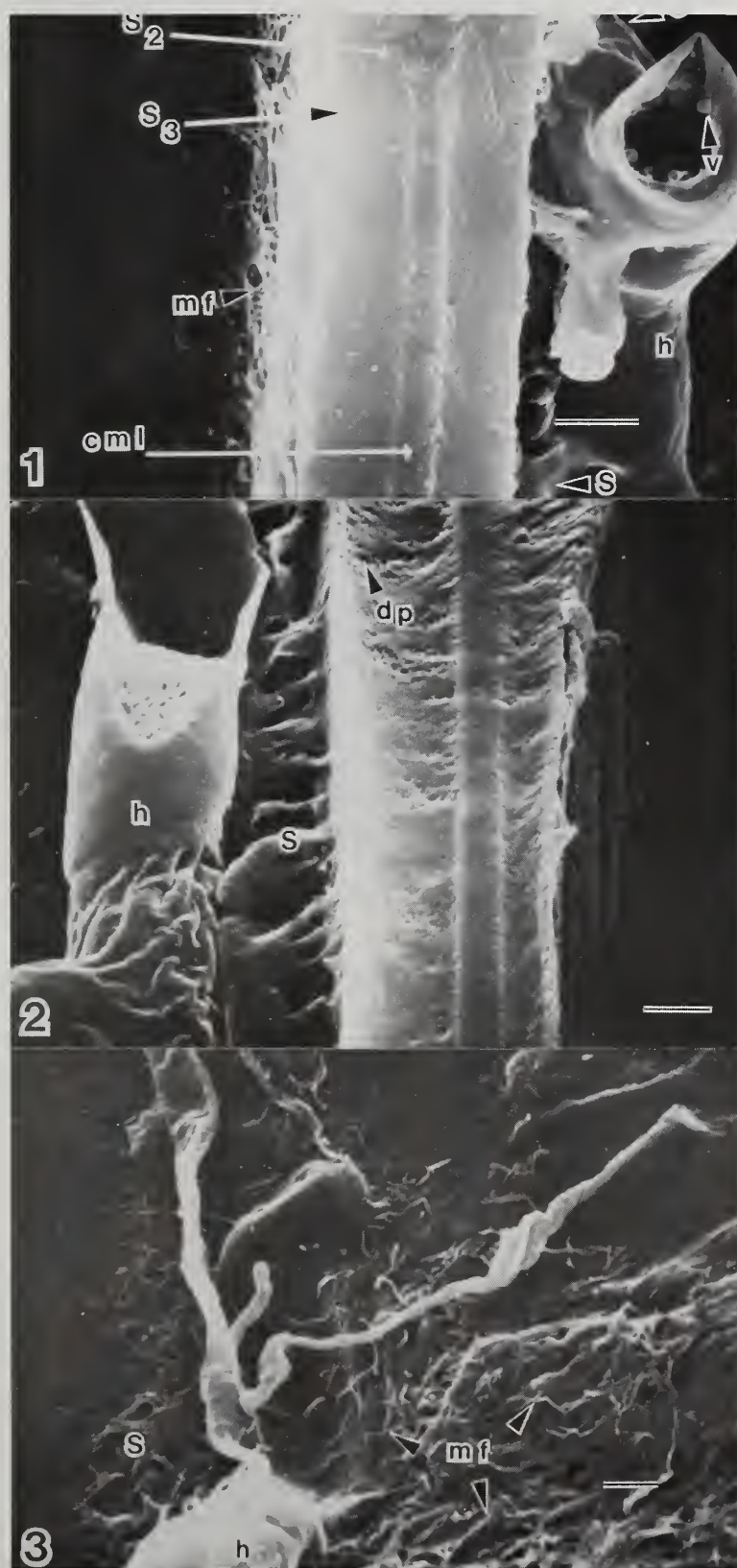
It is likely that this SEM study is not free from modification of biological structure due to the inherent nature of SEM preparative methodology. Nevertheless, we have purposely avoided the standard procedures of aqueous chemical fixation, alcohol dehydration and buffer washings which may have adverse effects on the morphology and interpretation of extracellular structures. Additional correlative studies using a variety of SEM and TEM preparative procedures will be required to confirm or disprove this model. However, our observations of wood and fungal structures during decay are strengthened by the application of two dissimilar fixation methods, i.e., quenching in liquid  $N_2$ -lyophilization and chemical fixation in  $OsO_4$  vapors. These interpretations might be invalid if the following can not be excluded: (a) microfracture planes or channels of decayed wood cell walls mimic penetrating mycofibrils, (b) structural artifacts arise from fixation and dehydration of existing woody structures, (c) dehydration results in modification or condensation of some extracellular hyphal structures, (d) disruption of hyphal integrity manifests extracellular membranous structures, or (e) sheath and/or membranous structures are modified lignin layers.

In conclusion, we have confirmed by SEM the presence of extracellular membranous, fibrous, and vesicular structures, previously designated as sheath, which appear to originate within the fungal cell wall. These

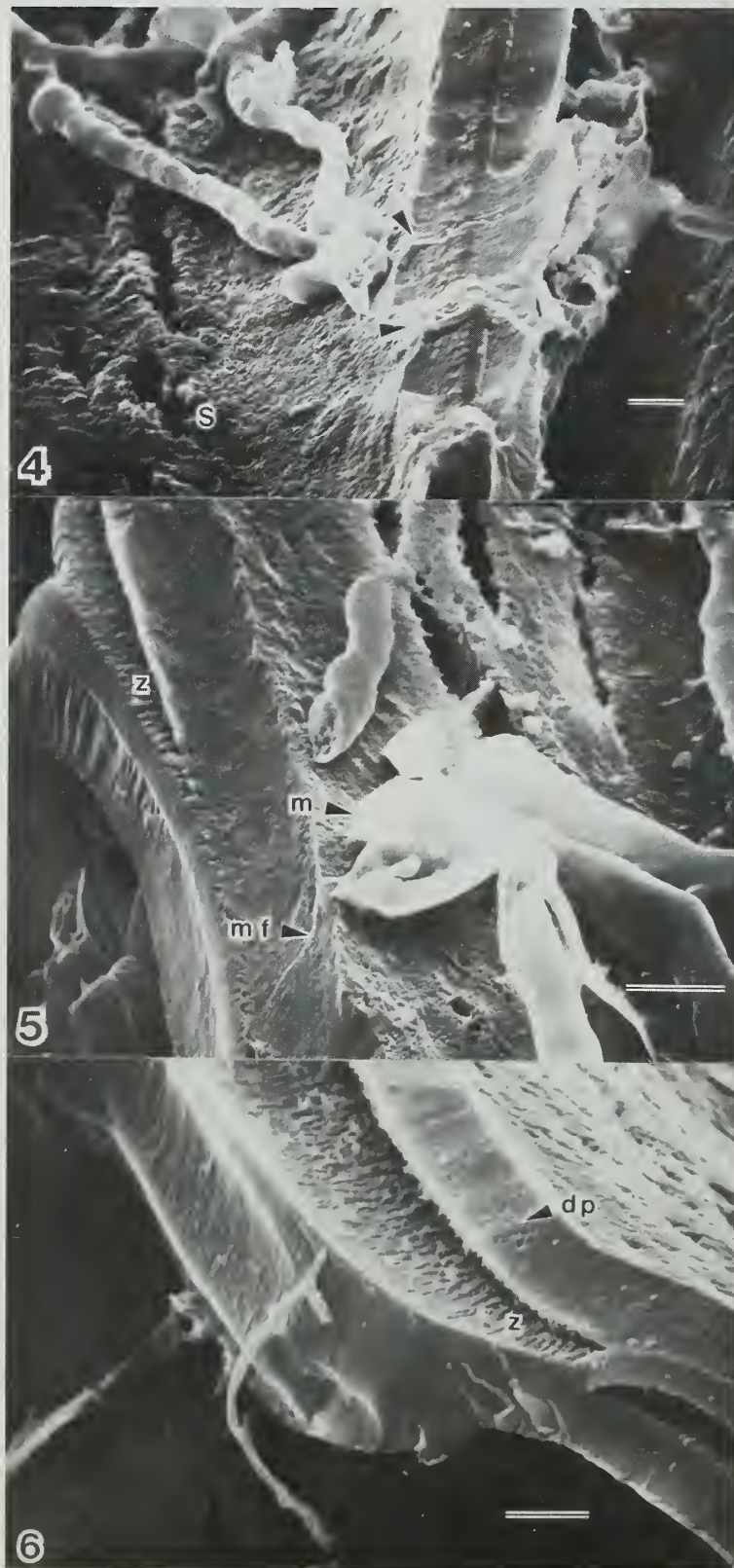
structures cover the  $S_3$  and penetrate all layers of the wood cell wall in a linear and progressive manner. Our proposed model depends upon additional confirmational evidence that the structures which appear to arise within the cell wall of the hyphae are the same structures which appear within the wood cell wall during decay by P. placenta.



Figures 1-3. *Postia placenta* on *Pinus* sp. quenched in liquid N<sub>2</sub> and lyophilized. Fig. 1. Longitudinally fractured surface with sheath (s) and vesicles (v) associated with hyphae (h) on surface of modified S<sub>3</sub>. Note mycofibrils on S<sub>3</sub> surface of adjacent tracheid (x 12,500). Fig. 2. Longitudinally fractured surface with hyphae (h) and sheath (s) attached to modified S<sub>3</sub>. Note linear arrangement of small decay pockets in S<sub>2</sub> and extending across compound middle lamella (cml) (x 10,000). Fig. 3. With hyphae (h), sheath (s), and branched mycofibrils on S<sub>3</sub> surface of tracheid (x 8,000; all bars = 1  $\mu$ m).



Figures 4-6. Longitudinal face of fractured Pinus sp. wood decayed by Postia placenta quenched in liquid  $N_2$  and lyophilized. Fig. 4. Intact hyphae of P. placenta in adjacent cell lumen penetrating cell wall layers from  $S_3$  to  $S_3$  by extracellular hyphal structures (arrows). Note the extensive development of the sheath (s) across the cell-wall surface (x 4,000). Fig. 5. Membranous structure (m) associated with hyphae on surface of  $S_3$  with mycofibrils extending from the membranous structure through the  $S_3$  into the  $S_2$  of the cell wall. Note small decay pockets in  $S_2$  associated with hyphae and the zone (z) of separation at the interface of the  $S_1$  and  $S_2$  (x 6,000). Fig. 6. Separation zone (z) at interface of  $S_1$  and  $S_2$  suggests preferential decay of this layer. Note decay pockets (dp) in  $S_2$  adjacent to  $S_3$  (x 6,000; all bars = 2  $\mu m$ ).





THE INTERNATIONAL RESEARCH GROUP ON WOOD PRESERVATION

Working Group I a

Biological Problems (Flora)

PROPOSED MODEL FOR THE PENETRATION AND DECAY OF WOOD BY  
THE HYPHAL SHEATH OF THE BROWN-ROT FUNGUS POSTIA PLACENTA.

by

F. Green, M. J. Larsen, L. L. Murmanis, and T. L. Highley

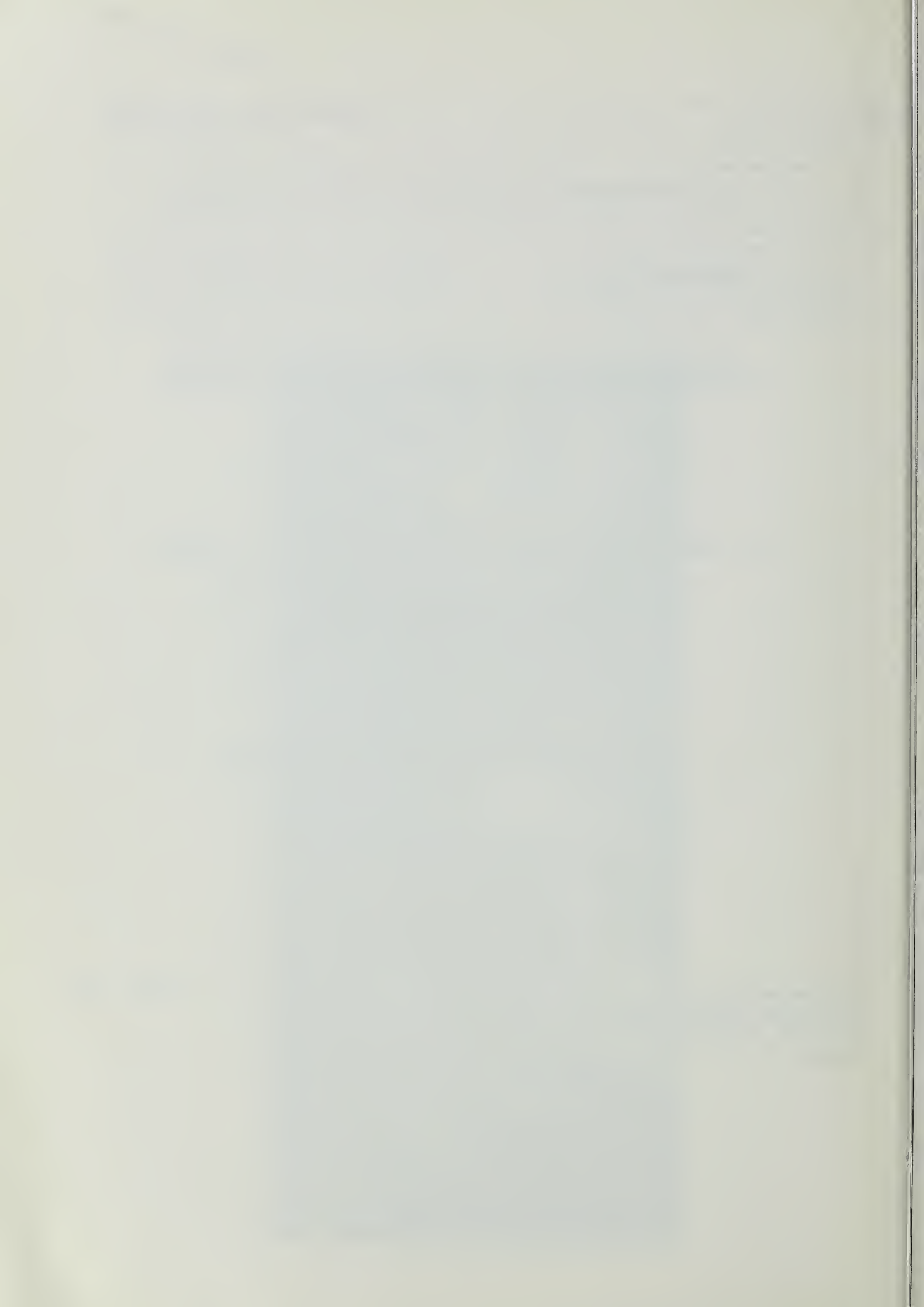
U.S. Department of Agriculture, Forest Service  
Forest Products Laboratory  
One Gifford Pinchot Drive  
Madison, Wisconsin, USA 53705-2398

Paper prepared for Twentieth Annual Meeting

Lappeenranta, Finland  
21-26, May 1989

IRG Secretariat  
Drottning Distinas vag 47 C  
S-114 28 Stockholm  
Sweden

4 March 1989





PROPOSED MODEL FOR THE PENETRATION AND DECAY OF WOOD  
BY THE HYPHAL SHEATH OF THE BROWN-ROT FUNGUS POSTIA PLACENTA.

By

Green, F., M.J. Larsen, L.L. Murmanis, and T.L. Highley  
U.S. Department of Agriculture, Forest Service  
Forest Products Laboratory<sup>1</sup>, Madison, WI, USA 53705-2398

SUMMARY

Scanning electron microscopy (SEM) of Pinus sp. decayed by the brown-rot fungus Postia placenta confirmed the existence of extracellular membranous structures previously described by transmission electron microscopy (TEM). These structures appear to be an integral part of the hyphal sheath and assume a variety of forms including lamellar sheets, fibrils, and vesicles. These structures were observed (a) on the surface of hyphae, (b) extending from hyphae onto the wood surface and covering the  $S_3$  layer, (c) embedded in the hyphal sheath and, (d) penetrating into the wood cell wall layers from  $S_3$ - $S_3$ .

We conclude that penetration of the wood cell wall by the complex, multistructured hyphal sheath facilitates the decay process in an orderly and linear progression. The directionality of the decay process appears to alter the fiber orientation of individual wood cell wall layers. This model offers an alternative hypothesis to simple diffusion of wood degrading agents during wood decay by P. placenta.

Keywords: Brown-rot, wood decay, hyphal sheath, extracellular membranous structures, wood anatomy, electron microscopy (SEM).

INTRODUCTION

Our current understanding of the ultrastructural micromorphology of wood-fungus interactions during wood decay, has been derived in large part from transmission electron micrographs (TEM) (12, 13, 19, 30, 33). Thus, observations have been restricted to a thin two-dimensional plane providing salient but limited information on the modifications of wood during the decay process. Questions specifically addressing enzyme penetration and decay progression have not been satisfactorily resolved by TEM (8, 30, 31, 32).

There is an apparent void in the literature between early observations on the decay fungi in wood by SEM and the present (4, 11, 14, 20, 21, 27). Many of the earlier papers present low magnification SEM micrographs limited to

---

<sup>1</sup>The Forest Products Laboratory is maintained in cooperation with the University of Wisconsin. This article as written and prepared by U.S. Government employees on official time, and it is therefore in the public domain and not subject to copyright.

surface phenomena of the  $S_3$ . The current availability of high resolution scanning electron microscopes, concurrent with improvements in creative methodology of SEM specimen preparation provides an additional correlate to TEM for ultrastructural studies. Application of SEM technology should confirm fungal and wood structures during decay previously detailed by TEM.

In a series of provocative publications Foisner et al. (12, 13) and Messner et al. (25, 26, 27) described in detail for the first time, using transmission electron microscopy, extracellular membranous structures (sheath) of brown- and white-rot basidiomycetes, and suggested a possible role for these structures in wood decay.

Extracellular layers (hyphal sheath) enveloping vegetative hyphae of fungi are a common morphological feature (2, 29). Hyphal sheaths are postulated to provide several functions for living hyphae; e.g., (a) attachment to solid substrates, (b) a nutrient reserve, (c) reduce dessication and nutrient loss, (d) provide protection against toxic chemicals, (e) facilitate wood degradation by storing or concentrating wood degrading agents, (f) maintain a favorable moisture/pH environment for enzyme activity, and (g) conditioning the substrate prior to enzyme action (17).

The results presented in this communication confirm by SEM the existence of extracellular membranous structures of the brown-rot fungus P. placenta, and penetration of wood cell-wall layers by these structures. These results also provide a supplemental mechanism to account for distribution of wood decay agents during brown-rot decay.

## MATERIALS AND METHODS

Wood blocks (8 x 8 x 4 mm) of southern yellow pine (Pinus sp.) were decayed by the brown-rot fungus Postia placenta (Fr.) M. Lars. et Lomb. (isolate no. MAD-698) using the ASTM soil-block procedure (1). At intervals during the 2-13 week decay period, selected blocks were removed and rapidly quenched in precooled (30 psi, -210C) liquid nitrogen ( $N_2$ ) without chemical fixation. After 15 minutes blocks were transferred to a precooled cryovessel and lyophilized overnight (ca. 12 hours). Blocks prepared in this manner were then split longitudinally with a razor blade to expose the radial face, and then coated with gold (Au) on a Balzer's sputter-coater for 22 sec. resulting in an Au-layer ca. 65-70 Å thick. Additional blocks were fixed by exposure to vapors of osmium tetroxide (1%) in an environmental hood, air dried, and gold coated as above. Specimens were observed with the aid of a Hitachi S-530 scanning electron microscope at an accelerating voltage of 20-25 Kv. Working distances were ca. 5-10 mm.



## RESULTS

Degradation of southern yellow pine (*Pinus* sp.) by the brown-rot fungus *Postia placenta* is shown in figures 1-21. Figures 1 and 2 illustrate fungal hyphae in close proximity to the longitudinally fractured faces of the tracheid cell wall. Extracellular hyphal structures extending from the hyphal cell wall can be seen attached to the modified  $S_3$  of the cell wall, with decay pockets visible in the  $S_2$  layer (Fig. 2).

The  $S_3$  surface layer of nearly all tracheids observed in this study was covered by  $S_3$  sheath matrix, thus obliterating the underlying wood fiber structure (Figs. 3-4). Although some tracheids examined contained more than one hypha, usually only a single hypha per tracheid appeared sufficient to mask the  $S_3$  surface with hyphal sheath and branched mycofibrils.

As decay progresses, linear penetration by mycofibrils across the  $S_3$  and into the  $S_2$  is observed extending from areas covered by hyphae and extracellular hyphal sheath, especially in close proximity to hyphae and hyphal sheath structures (Figs. 4-5). The mycofibrillar penetrations into cell walls resemble the structures of the modified  $S_3$  and penetrate radially from  $S_3$  to opposing  $S_2$  of adjacent tracheid walls. Prior to tangential penetration by mycofibrils into the  $S_2$ , preferential hydrolysis of the  $S_1$ - $S_2$  interface zone (z) of the wood cell wall was observed (Figs. 5-6). Microfibrils, similar in size to mycofibrils, are visible within this decay zone.

Extracellular hyphal structures are variable in size and configuration. Figures 7 and 8 illustrate branched, fused and vesicular manifestations of the hyphal sheath. Figure 9 demonstrates mycofibrils (approx. 50 nm in diam.) on a "hairy" hypha in contact with the wood cell surface. Hyphal sheath is also observed as a smooth bilayer overlaying the mycofibrils which arise from the fungal cell wall layer underneath the sheath (Fig. 10). Both sheath and fungal cell wall-associated mycofibrils extend onto the surface of the  $S_3$  and are shown fusing into a uniform and ubiquitous structure (Figs. 11-12).

Mycofibrillar structures are shown penetrating the modified  $S_3$  and  $S_2$  radially. The apparent orientation of the  $S_3$  layer now follows the radial penetration of the sheath mycofibrils. The radial orientation continues through the compound middle lamellae into the opposing cell wall (Figs. 13-15). Decay pockets in the radial plane also reveal mycofibrillar orientation to  $S_1$ - $S_2$  interface. The preferential hydrolysis of the  $S_1$ - $S_2$  interface (z) visible on the oblique surface (os) is obscured by mycofibrils or sheath on the longitudinal surface (ls) (Fig. 15). A membranous remnant, apparently bilayered, is visible (Fig. 15). Penetration of the  $S_2$  is evidenced by membranous and fibrillar sheath elements which extend from the  $S_3$  (Fig. 16). Mycofibrils and branched decay channels within the  $S_2$  and bridging the wood cell wall are evident in Figure 17. Fibrous sheath is visible within the tracheid lumen and continues linearly through the  $S_2$  layer of the opposing wood cell wall (Fig. 18). Additional representations of the extracellular membranous structures (m) are shown in apposition to modified  $S_3$  of the wood cell wall (Figs. 19, 20 and 21).

## DISCUSSION

Extracellular membranous and fibrillar structures were visualized by SEM extending from the hyphal cell wall and penetrating wood cell wall layers. These hyphal sheath structures provide an alternative model to account for



transport of wood degrading agents during decay progression. This model also provides a means for the uptake and transport of nutrients to the fungal protoplasts. The primary barrier to the existing simple diffusion model to explain the movement of wood decay enzymes has been the apparent lack of appropriately sized pores in cell wall layers required to permit diffusion of enzymes of the 30-60 kD range (15, 23, 24, 33, 34) even after decay has been initiated. Therefore, a low molecular weight, non-enzymatic system was postulated (23). The sheath may be necessary to predispose the cell wall layers, especially the modification of the  $S_2$ , as a prerequisite for penetration of decay enzymes. Furthermore, decay pores and channels may be progressively obstructed by sheath structures during decay, thus blocking simple diffusion.

Many of the underlying concepts and structures supporting this proposed model of penetration of decay agents by hyphal sheath components already exist in the literature. Numerous authors have suggested a role in fungus-host interactions for penetration hyphae, appressoria, haustoria, needle-like infection hyphae, and microhyphae (2, 10, 16, 24, 35). In a review of wood decay, Liese (24) illustrated "mycofibrils" of Chaetomium globosum Kunze, and suggested a role for these structures in penetration and decay. We concur with the use of the term 'mycofibril' to designate the structure observed here. We also propose consideration of the analogous term 'mycovesicle' to designate membranous vesicles exterior to the hyphal plasmalemma. Foisner et al. (12, 13) and Messner et al. (25, 26, 27) described hyphal cell wall systems and tripartite extracellular membranous structures of brown- and white-rot fungi. We conclude that the structures reported here from SEM are essentially the same as those reported in their studies. From TEM it is known that the hyphal sheath extends some distance away from the hyphae (12, 18, 25, 26, 29, 30), and is confirmed here by SEM. Wood decay, especially brown-rot, occurs in a ubiquitous fashion in the wood cell wall at great distances from the hyphae (4, 17, 18). Apparently, the small structures observed extending into the wood cell wall are difficult to resolve in TEM, possibly due to chemical modification during specimen preparation, elution or their inherent low electron density (electron lucent) in wood (2). Low molecular weight polysaccharides, such as water soluble b-1,3 (1,6) glucans, are known to be components of the hyphal sheath (17).

It is our understanding from TEM and SEM that mycofibrils and mycovesicles are modifications of the hyphal plasmalemma, similar to lomasomes (2), which arise in the periplasmic space of the hyphal cell (unpublished results). We propose that the fundamental unit of the extracellular hyphal sheath is the mycovesicle that can self-assemble within the fungal cell wall and coalesce to form a fluid and dynamic assemblage of extracellular structures (13). In concert with this perspective, we have observed that mycovesicles and mycofibrils appear to coalesce into lamellar sheets and dedifferentiate into mycovesicles and mycofibrils during penetration of the wood cell wall. Sheath membranes, therefore, are probably "self-assembled" from large numbers of mycovesicles and mycofibrils (13). Foisner et al. (13) further characterized tripartite extracellular membranes biochemically as containing carbohydrate, lipid, and protein but without phospholipid. They concluded that these membranes are functionally different from plasma membranes. Bracker (3), reporting on Gilbertella, provided convincing evidence for the ability of biomembranes to undergo numerous morphological transformations, e.g., "vesicles, tubes, or sheets." We view the intracellular representations of Bracker's membranes as analogous to the extracellular hyphal sheath structures described here.



Inherent in the wood decay process is an intimate relationship between the underlying physical and biochemical structure of the wood cell wall and degradation by decay agents of Postia placenta. In this SEM study, the microfibrillar structure of decayed wood is modified by sheath structures. The estimated hemicellulose content of the  $S_3$ ,  $S_2$  matrix,  $S_1$ , CML and cell corners parallels sites of initial attack by P. placenta (9, 18, 31). Lignin is not an obvious chemical barrier to brown-rot decay by P. placenta, despite the apparent absence of lignin-specific enzymes that are formed in white rot fungi (e.g. Phanerochaete chrysosporium Burds. in Burds. et Eslyn). Brown-rot fungi have been reported to demethylate lignin resulting in an accumulation of polymeric degradation products (22). All cell wall layers are penetrated with rapid removal of hemicellulose (6, 17). Hemicellulose content is high at the  $S_1$ - $S_2$  and  $S_2$ - $S_3$  interfaces (32), predisposing the cell wall to preferential hydrolysis at these interfaces. A similar pattern of selective decay has been reported for Schizophyllum commune Fr. on Pinus sylvestris L. (7). However, in our study the rapid hydrolysis at the  $S_1$ - $S_2$  interface may also be explained by direct penetration by decay agents from transverse surfaces of colonized wood blocks.

Decay of the compound middle lamella and penetration of hyphae into cell wall corners has been previously reported using TEM (18). The mechanisms by which P. placenta modify or oxidize lignin during removal of hemicellulose and cellulose remains obscure (18, 22). Subsequent reagglomeration or precipitation of modified lignin residues appears similar to residues which remain following enzyme hydrolysis and steam explosion (9,10). Fracture faces of decayed and dehydrated wood blocks are most likely to occur in the weakest planes. Thus, selective decay and penetration of existing wood cell-wall structure by P. placenta apparently reveals underlying physical or chemical structure not evident in undecayed control blocks (unpublished results). Progressive penetration of Pinus wood by P. placenta appears linear and perpendicular to the tracheid cell wall. This directionality of decay penetration has been previously documented by TEM (18, 32). Some anatomical features of wood structure revealed by P. placenta appear similar to those observed in Douglas-fir following removal of cellulose and hemicellulose by hydrofluoric acid (5).

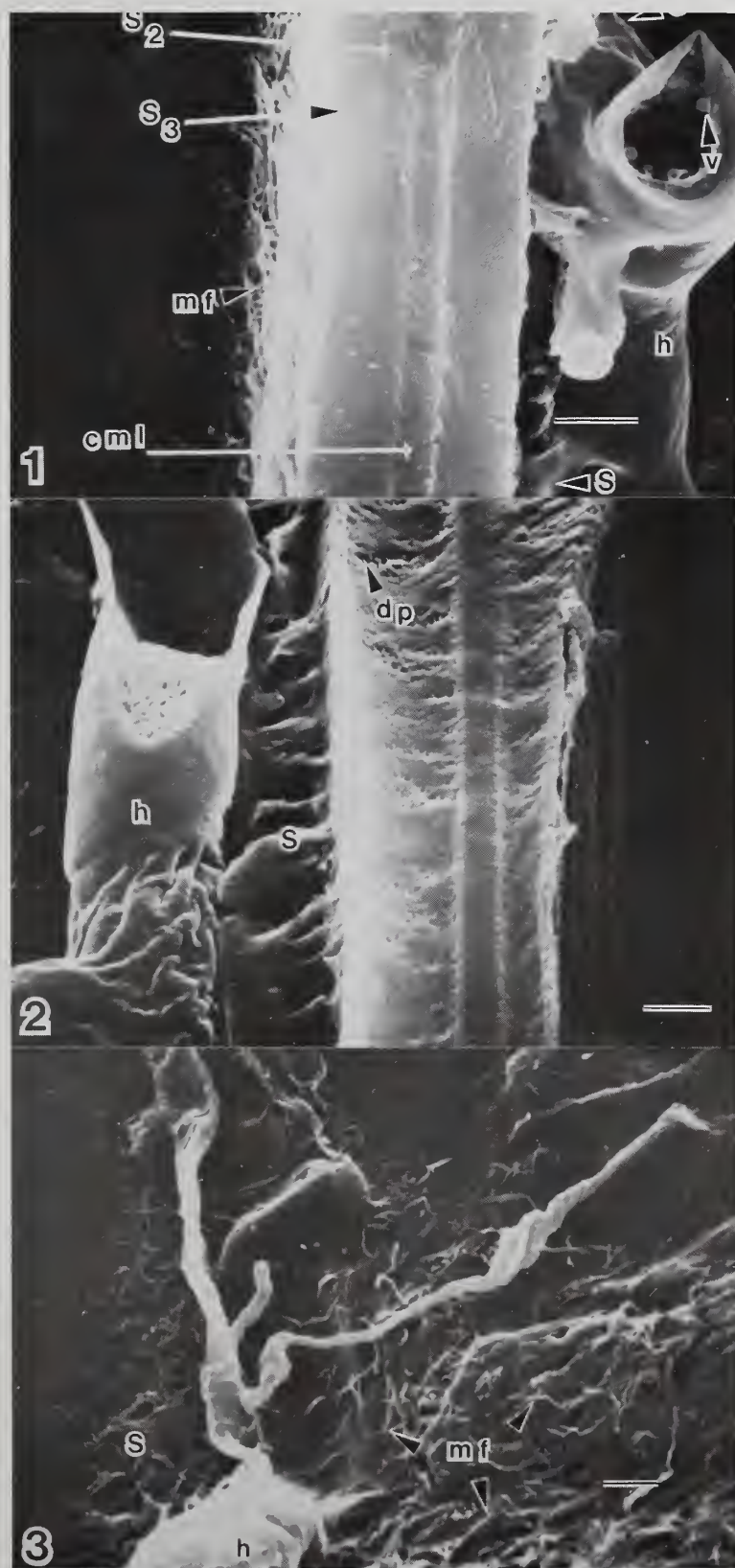
It is likely that this SEM study is not free from modification of biological structure due to the inherent nature of SEM preparative methodology. Nevertheless, we have purposely avoided the standard procedures of aqueous chemical fixation, alcohol dehydration and buffer washings which may have adverse effects on the morphology and interpretation of extracellular structures. Additional correlative studies using a variety of SEM and TEM preparative procedures will be required to confirm or disprove this model. However, our observations of wood and fungal structures during decay are strengthened by the application of two dissimilar fixation methods, i.e., quenching in liquid  $N_2$ -lyophilization and chemical fixation in  $OsO_4$  vapors. These interpretations might be invalid if the following can not be excluded: (a) microfracture planes or channels of decayed wood cell walls mimic penetrating mycofibrils, (b) structural artifacts arise from fixation and dehydration of existing woody structures, (c) dehydration results in modification or condensation of some extracellular hyphal structures, (d) disruption of hyphal integrity manifests extracellular membranous structures, or (e) sheath and/or membranous structures are modified lignin layers.

In conclusion, we have confirmed by SEM the presence of extracellular membranous, fibrous, and vesicular structures, previously designated as sheath, which appear to originate within the fungal cell wall. These

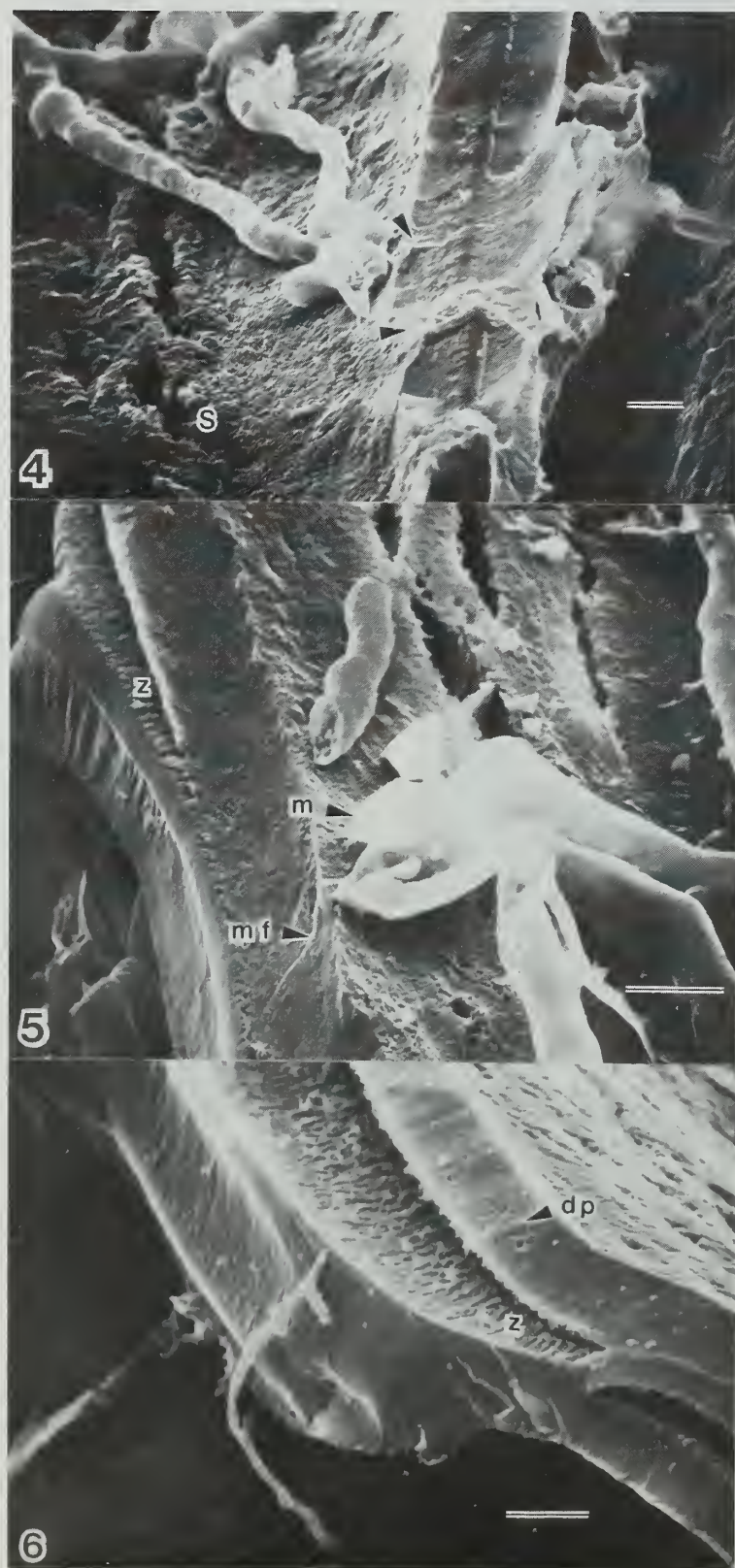
structures cover the  $S_3$  and penetrate all layers of the wood cell wall in a linear and progressive<sup>3</sup> manner. Our proposed model depends upon additional confirmational evidence that the structures which appear to arise within the cell wall of the hyphae are the same structures which appear within the wood cell wall during decay by P. placenta.



Figures 1-3. *Postia placenta* on *Pinus* sp. quenched in liquid N<sub>2</sub> and lyophilized. Fig. 1. Longitudinally fractured surface with sheath (s) and vesicles (v) associated with hyphae (h) on surface of modified S<sub>3</sub>. Note mycofibrils on S<sub>3</sub> surface of adjacent tracheid (x 12,500). Fig. 2. Longitudinally fractured surface with hyphae (h) and sheath (s) attached to modified S<sub>3</sub>. Note linear arrangement of small decay pockets in S<sub>2</sub> and extending across compound middle lamella (cml) (x 10,000). Fig. 3. With hyphae (h), sheath (s), and branched mycofibrils on S<sub>3</sub> surface of tracheid (x 8,000; all bars = 1  $\mu$ m).

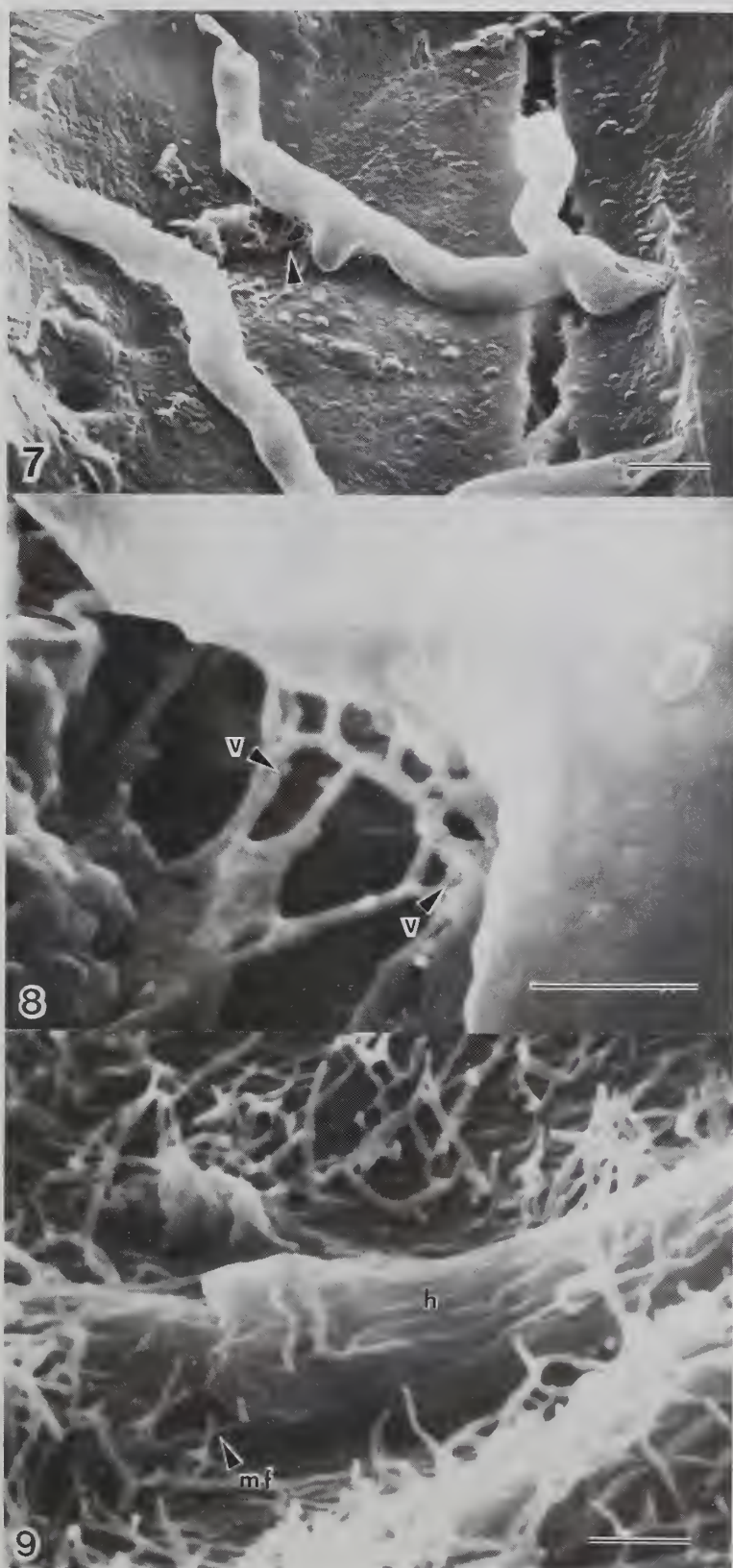


Figures 4-6. Longitudinal face of fractured Pinus sp. wood decayed by Postia placenta quenched in liquid N<sub>2</sub> and lyophilized. Fig. 4. Intact hyphae of P. placenta in adjacent cell lumen penetrating cell wall layers from S<sub>3</sub> to S<sub>2</sub> by extracellular hyphal structures (arrows). Note the extensive development of the sheath (s) across the cell-wall surface (x 4,000). Fig. 5. Membranous structure (m) associated with hyphae on surface of S<sub>3</sub> with mycofibrils extending from the membranous structure through the S<sub>3</sub> into the S<sub>2</sub> of the cell wall. Note small decay pockets in S<sub>2</sub> associated with hyphae and the zone (z) of separation at the interface of the S<sub>1</sub> and S<sub>2</sub> (x 6,000). Fig. 6. Separation zone (z) at interface of S<sub>1</sub> and S<sub>2</sub> suggests preferential decay of this layer. Note decay pockets (dp) in S<sub>2</sub> adjacent to S<sub>3</sub> (x 6,000; all bars = 2  $\mu$ m).

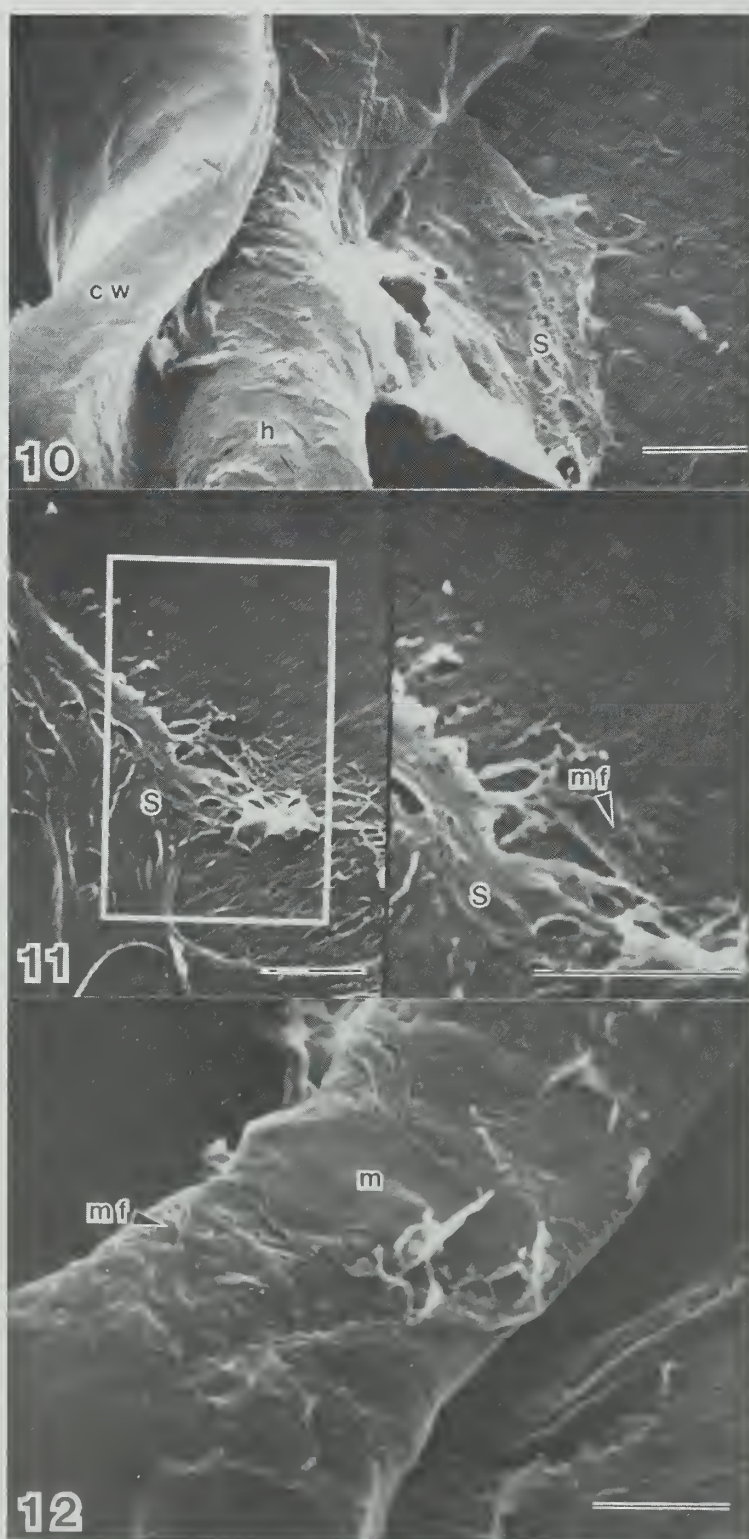




Figures 7-9. Extracellular extensions of the hyphal cell wall of P. placenta (Figs. 7-8, quenched in liquid N<sub>2</sub> and lyophilized). Fig. 7. Hyphae extending across tracheid lumen with hyphal sheath components extending from hypha to cell wall surface. Note what appears to be a hyphal track extending underneath intact hyphae to a bore hole (lower left) (x 6,000; bar = 2 um). Fig. 8. Increased magnification of portion of Fig. 7 depicting branched mycofibrils and vesicle-like structures (x 50,000; bar = 0.5 um). Fig. 9. Collapsed hyphae (h) bearing mycofibrils (mf) that are extending onto S<sub>2</sub> surface. The membranous part of the sheath appears to be absent (x 30,000; bar = 0.5 um; fixed in OsO<sub>4</sub> vapors and air dried).

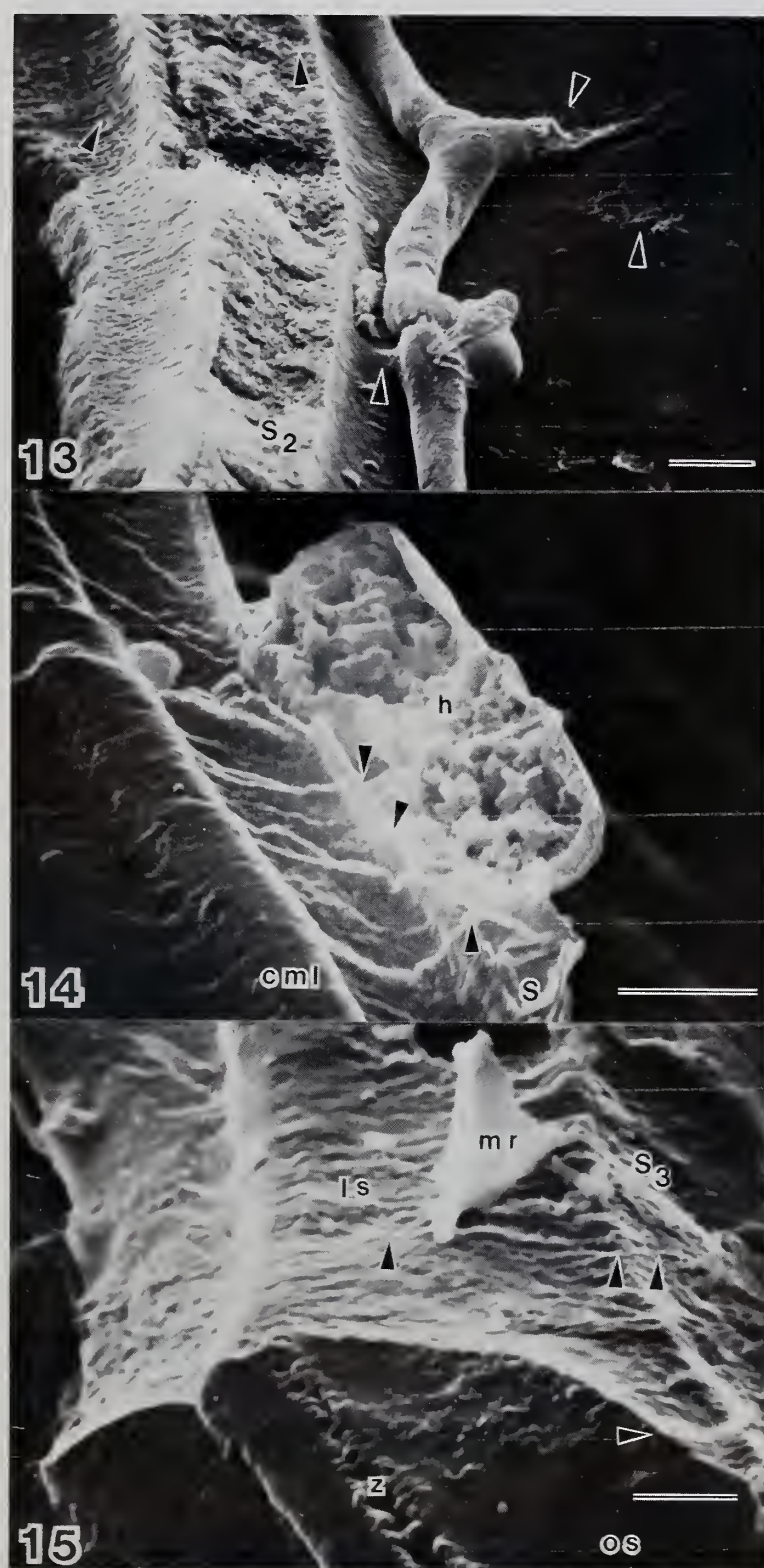


Figures 10-12. Extracellular hyphal sheath associated with hyphae and surface of  $S_3$  (quenched in liquid  $N_2$  and lyophilized). Fig. 10. Hypha juxtaposed to wood cell wall (cw) with sheath (s) extending from hypha (h) to surface of  $S_3$ . Note the fibrillar surface of hypha ( $\times 15,000$ ). Fig. 11. Overlying membrane of sheath (s) revealing underlying mycofibrils (mf) in contact with  $S_3$  ( $\times 15,000$  and  $\times 30,000$ , respectively). Fig. 12. Hypha with a membrane-like outer cell wall covering (m) associated with underlying mycofibrils. Note that both layers appear to have been attached to the modified  $S_3$  ( $\times 20,000$ ; all bars = 1  $\mu m$ ).



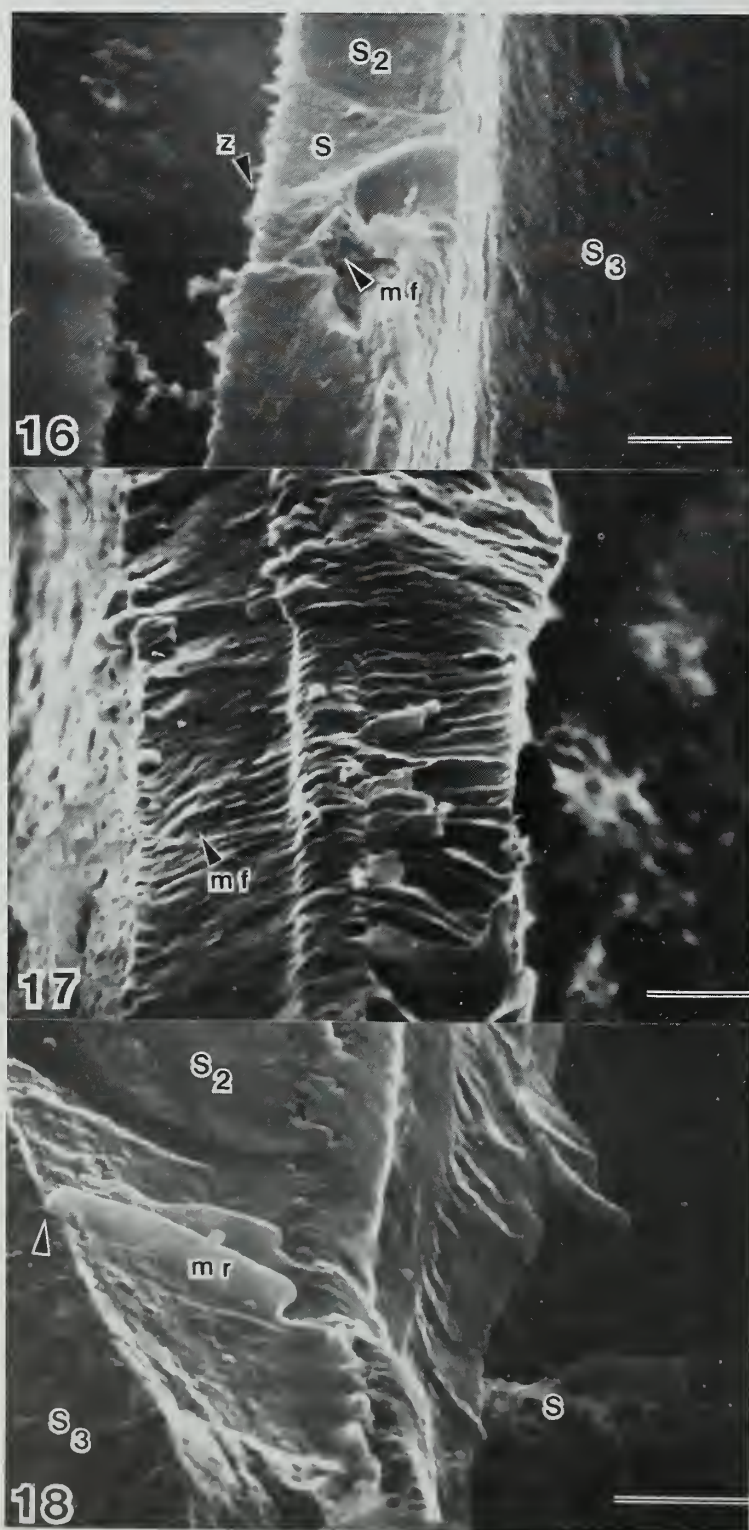


Figures 13-15. Longitudinal fracture face of pine showing linear penetration of wood cell wall by extracellular mycofibrils of *P. placenta* (quenched in liquid  $N_2$  and lyophilized). Fig. 13. Hyphae in tracheid lumen. Mycofibrils (arrows) can be seen on the hypha, on the surface of the  $S_3$ , extending from hypha to  $S_3$ , and on the surface of the  $S_1$  of an adjacent tracheid. Note the linearity of the decay pattern in the  $S_2$  ( $\times 6,000$ ; bar = 2  $\mu m$ ). Fig. 14. Fractured hyphae (h) in direct contact with the  $S_3$  of tracheid and associated extracellular sheath (s). Mycofibrils (arrows) have penetrated the modified  $S_3$  perpendicular to the lumen, across the  $S_2$ ,  $S_1$ , and compound middle lamella ( $\times 20,000$ ; bar = 1  $\mu m$ ). Fig. 15. Corner of fractured cell wall formed by longitudinal (ls) and oblique (os) surface. Mycofibrils (arrows) are shown extending from the  $S_3$  into the  $S_2$  on both surfaces. A bilayered membrane remnant (mr) is also shown. Zone of separation (z) at  $S_1$ - $S_2$  interface is visible only on the os near decay pockets ( $\times 15,000$ ; all bars = 1  $\mu m$ ).

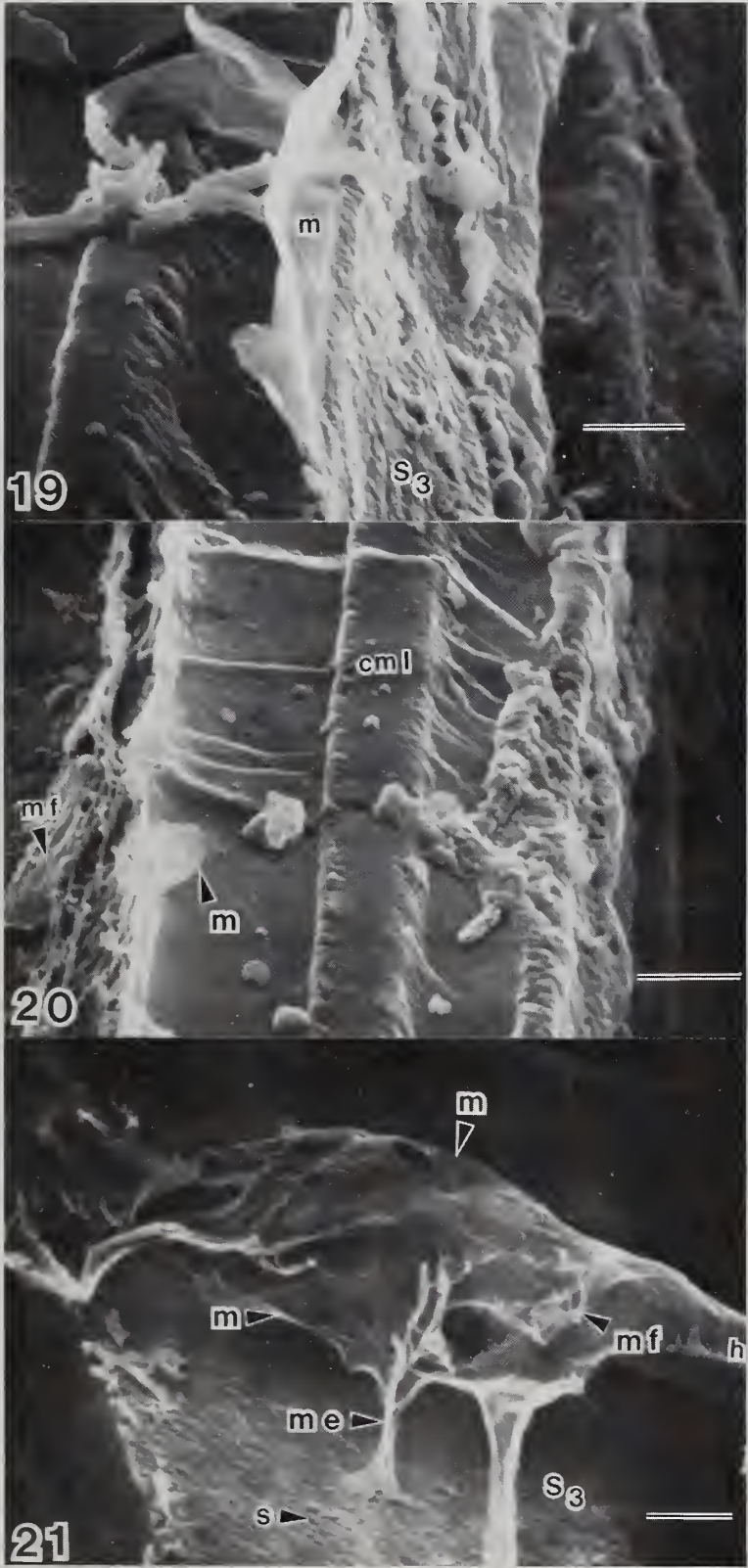




Figures 16-18. Fungal sheath components in longitudinal fracture faces of cell wall of *Pinus* decayed by *P. placenta* (quenched in liquid N<sub>2</sub> and lyophilized). Fig. 16. Penetration from modified S<sub>3</sub> into S<sub>2</sub> by mycofibrils (mf) associated with a putative membranous-like structure of the sheath (s). The zone of separation (z) is apparent at the S<sub>1</sub>-S<sub>2</sub> interface (x 15,000). Fig. 17. Topography of a longitudinally fractured cell wall. Note linear orientation of areas of penetration by mycofibrils (mf). Modified S<sub>3</sub> is apparent at left (x 15,000). Fig. 18. Sheath (s) extending through lumen space in linear apposition to membrane remnants (mr) in S<sub>2</sub> and compound middle lamella. Mycofibrils are evident at arrow (x 20,000; all bars = 1  $\mu$ m).



Figures 19-21. Longitudinal fracture of decayed *Pinus* sp. (quenched in liquid N<sub>2</sub> and lyophilized). Figs. 19-20. Penetration of cell wall by mycofibrils (mf) and membranous-like structures. Note apparent tri-lamellar nature of membranous fragment attached to modified S<sub>3</sub> (m) (x 15,000). Fig. 21. Extracellular membrane (m) extending from hyphae (h) to S<sub>3</sub> surface. Note the morphology of the membrane extension (me) in direct contact with modified S<sub>3</sub>. Mycofibrils (mf) can be readily seen in association with membrane (x 12,500; all bars = 1  $\mu$ m)





## REFERENCES

- [1] American Society for Testing and Materials (1971) Standard method for accelerated laboratory test of natural decay resistance of woods. ASTM Desig. D 2017, Philadelphia, Pa.
- [2] Bracker, C E (1967) Ultrastructure of fungi. Ann Rev Phytopath 5: 343-374
- [3] Bracker, C E (1968) The ultrastructure and development of sporangia in Gilbertella persicaria. Mycologia 60: 1016-1067
- [4] Bravery, A F (1977) The application of scanning electron microscopy in the study of timber decay. J Inst Wood Science 5: 13-19
- [5] Cote, W A (1967) Wood ultrastructure. An atlas of electron micrographs. Univ Washington Press
- [6] Cowling, E B (1965) Microorganism and microbial enzyme systems as selective tools in wood anatomy. In, Cote, W, ed., Cellular Ultrastructure of Woody Plants, pp. 341-368. Syracuse Univ Press
- [7] Daniel, G F, Nilsson, T (1984) Studies on the S<sub>2</sub> layer of Pinus silvestris. Report 154, The Swedish University of Agricultural Sciences UPSALA Sweden 1-37
- [8] Daniel, G F, Nilsson, T, and Pettersson, B (1988) Immunolabelling studies on the detection of enzymes during the degradation of wood by Phanerochaete chrysosporium. Inter Res Group On Wood Preserv Document No: IRG/WP/1364
- [9] Donaldson, L A (1988) Ultrastructure of wood cellulose substrates during enzymatic hydrolysis. Wood Sci Technol 22: 33-41
- [10] Donaldson, L A, Wong, K K Y, and Mackis, K L (1988) Ultrastructure of steam-exploded wood. Wood Sci Technol 22: 103-114
- [11] Eriksson, K E, Grunewald, A, Nilsson, T, and Vallander, L (1980) The scanning electron microscopy study of the growth and attack on wood by three white-rot fungi and their cellulase-less mutants. Holzforschung 34: 207-213
- [12] Foisner, R, Kessner, K, and Roehr, M. (1985) Wood decay by basidiomycetes: extracellular tripartite membranous structures. Trans Brit Mycol Soc 85: 257-266
- [13] Foisner, R, Messner, K, Stachelberger, H, and Roehr, M (1985) Isolation and characterization of extracellular three-lamellar structures of Sporotrichum pulverulentum. J Ultrastruct Res 92: 36-46
- [14] Goodell, B, Daniel, G, Jellison, J, and Nilsson, T (1988) Immunolocalization of extracellular metabolites from Poria placenta. Inter Res Group On Wood Preserv Document No: IRG/WP/1361

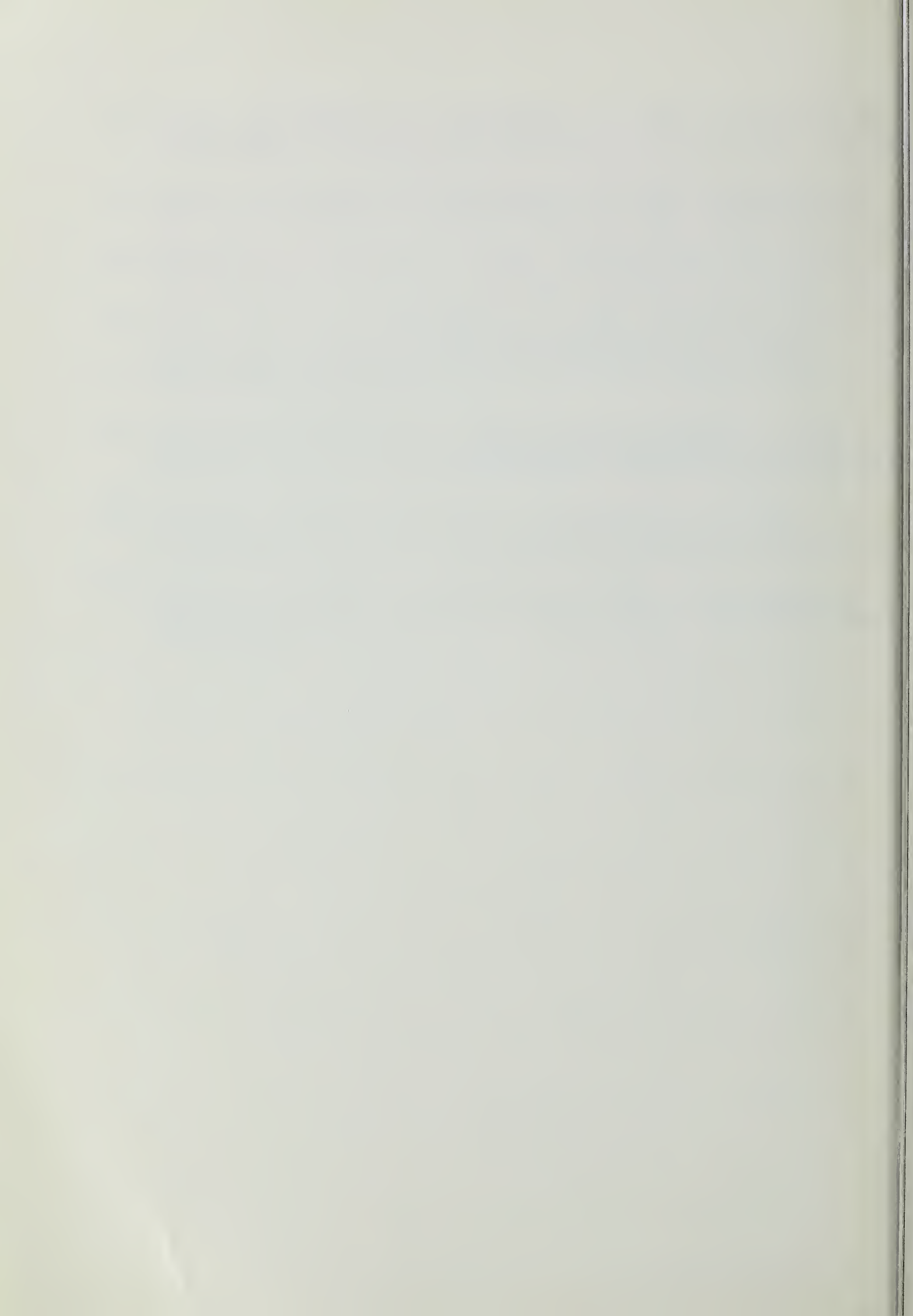


- [15] Green, F, Clausen, C A, Micales, J A, Highley, T L, and Wolter, K E (1989) Carbohydrate-degrading complex of the brown rot fungus Postia placenta: Purification of B-1,4 xylanase. Holzforschung 43: 25-32
- [16] Hickman, C J (1965) Fungal structure and organization. In, Ainsworth, C G and Sussman, A S, eds., The Fungi - An Advanced Treatise (Vol. 1) pp. 21-45. Academic Press
- [17] Highley, T L (1987) Biochemical aspects of white-rot and brown-rot decay. Inter Res Group On Wood Preserv Document No: IRG/WP/1319
- [18] Highley, T L, and Murmanis, L L (1985) Micromorphology of degradation in western hemlock and sweet gum by the brown-rot fungus Poria placenta. Holzforschung 39: 73-78
- [19] Highley, T L, and Murmanis, L L (1987) Micromorphology of degradation in western hemlock and sweet gum by the white-rot fungus Coriolus versicolor. Holzforschung 41: 67-71
- [20] Jutte, G M, and Sachs, I B (1976) SEM observations of brown-rot fungus Poria placenta in normal and compression wood of Picea abies. In, Scanning electron microscopy, Pt. VII, Proc Workshop Plant Science App., pp. 535-542. Ill Res Inst, Chicago
- [21] Jutte, S M, and Zabel, R A (1974) Initial wood decay stages as revealed by scanning electron microscopy. In, Scanning electron microscopy, Pt. II, Proc Workshop Plant Science, pp. 445-452. Ill Res Inst, Chicago
- [22] Kirk, T K (1975) Effects of a brown-rot fungus, Lenzites trabea, on lignin in spruce wood. Holzforschung 29: 99-107
- [23] Koenigs, J W (1974) Hydrogen peroxide and iron: A proposed system for decomposition of wood by brown-rot basidiomycetes. Wood and Fiber 6: 66-79
- [24] Liese, W (1970) Ultrastructural aspects of woody tissue disintegration. Ann Rev Phytopath 8: 231-258
- [25] Messner, K and Stachelberger, H (1984) Transmission electron microscope observations of brown-rot fungi caused by Fomitopsis pinicola with respect to osmiophilic particles. Trans Br Mycol Soc 83: 113-130
- [26] Messner, K and Stachelberger, H (1984) Transmission electron microscope observations of white-rot caused by Trametes hirsuta with respect to osmiophilic particles. Trans Brit Mycol Soc 83: 209-216
- [27] Messner, K, Srebotnik, E, Ertler, G, Foisner, R, Pettersson, B, and Stachelberger, H (1987) Cell wall systems, extracellular membranous structures and ligninase of wood rotting fungi. In, Lignin Enzymic and Microbial Degradation, pp. 243-249. Paris
- [28] Murmanis, L L, and Highley, T L (1987) Cytochemical localization of cellulases in decayed and nondecayed wood. Wood Sci Technol 21: 101-109

- [29] Palmer, J G, Murmanis, L L, and Highley, T L (1983) Visualization of hyphal sheath in wood-decay hymenomycetes. I. Brown rotters. *Mycologia* 75: 995-1004
- [30] Palmer, J G, Murmanis, L L, and Highley, T L (1984) Observations of wall-less protoplasts in white- and brown-rot fungi. *Mater Org* 19: 39-44
- [31] Parameswaran, N, and Liese, W (1982) Ultrastructural localization of wall components in wood cells. *Holz Reh- und Werkst* 40: 145-155
- [32] Ruel, K, Barnoud, F, and Eriksson, K E (1981) Micromorphological ultrastructural aspects of spruce wood degradation by wild type Sporotrichum pulverulentum and its cellulase-less mutant cell 44. *Holzforschung* 35: 157-171
- [33] Srebotnik, E, and Messner, K (1988) Spatial arrangement of lignin peroxidase in pine decayed by Phanerochaete chrysosporium and Fomitopsis pinicola. Inter Res Group On Wood Preserv Document No: IRG/WP/1343
- [34] Srebotnik, E, Messner, K, Foissner, R, and Pettersson, B (1988) Ultrastructural localization of ligninase of Phanerochaete chrysosporium by immunogold labeling. *Current Microbiol* 16: 221-227
- [35] Tsuneda, A, Koshitani, H, and Furukawa, I (1987) Micromorphological patterns of incipient wood decay by Lentinus edodes. Rept Tottori Mycol Inst 25: 36-48

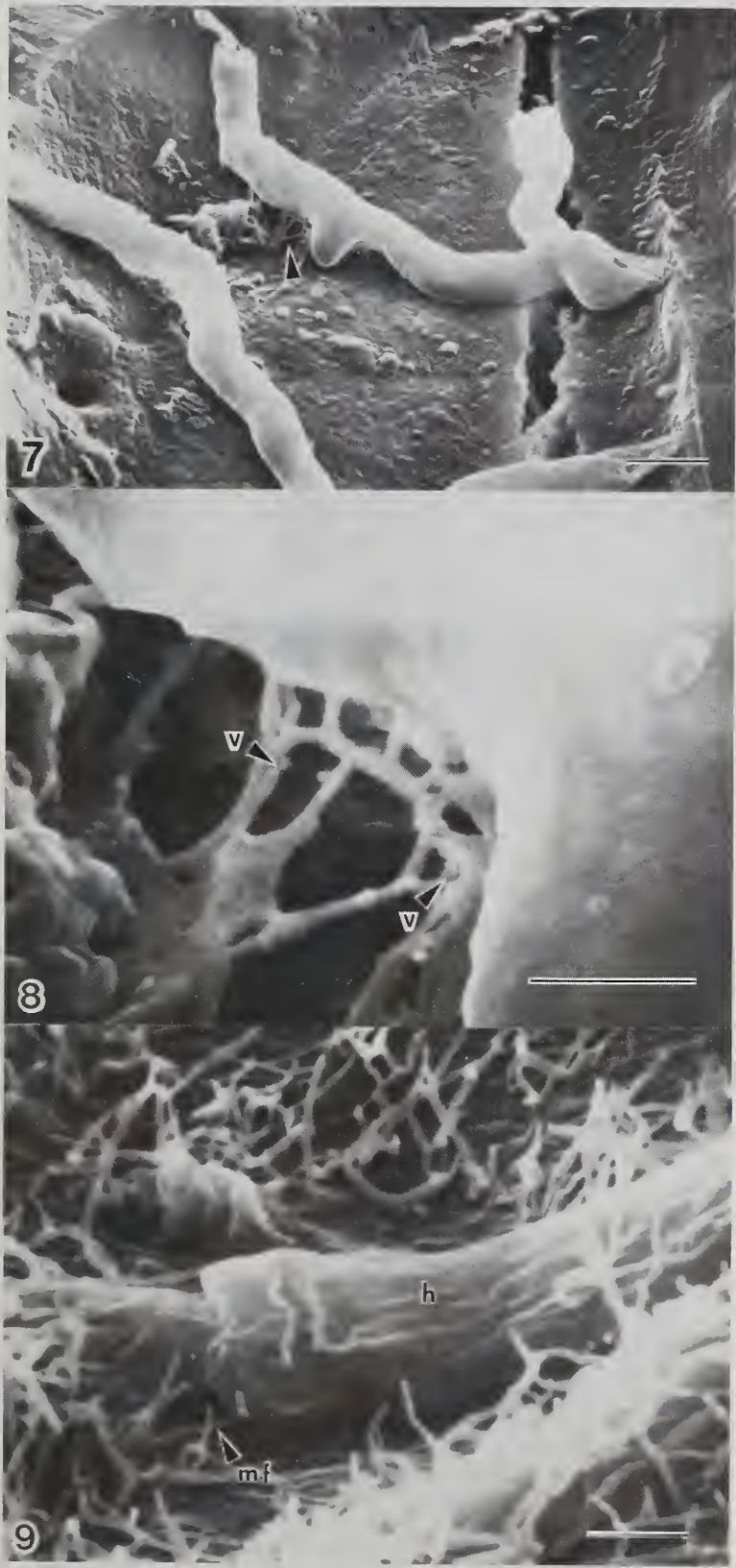




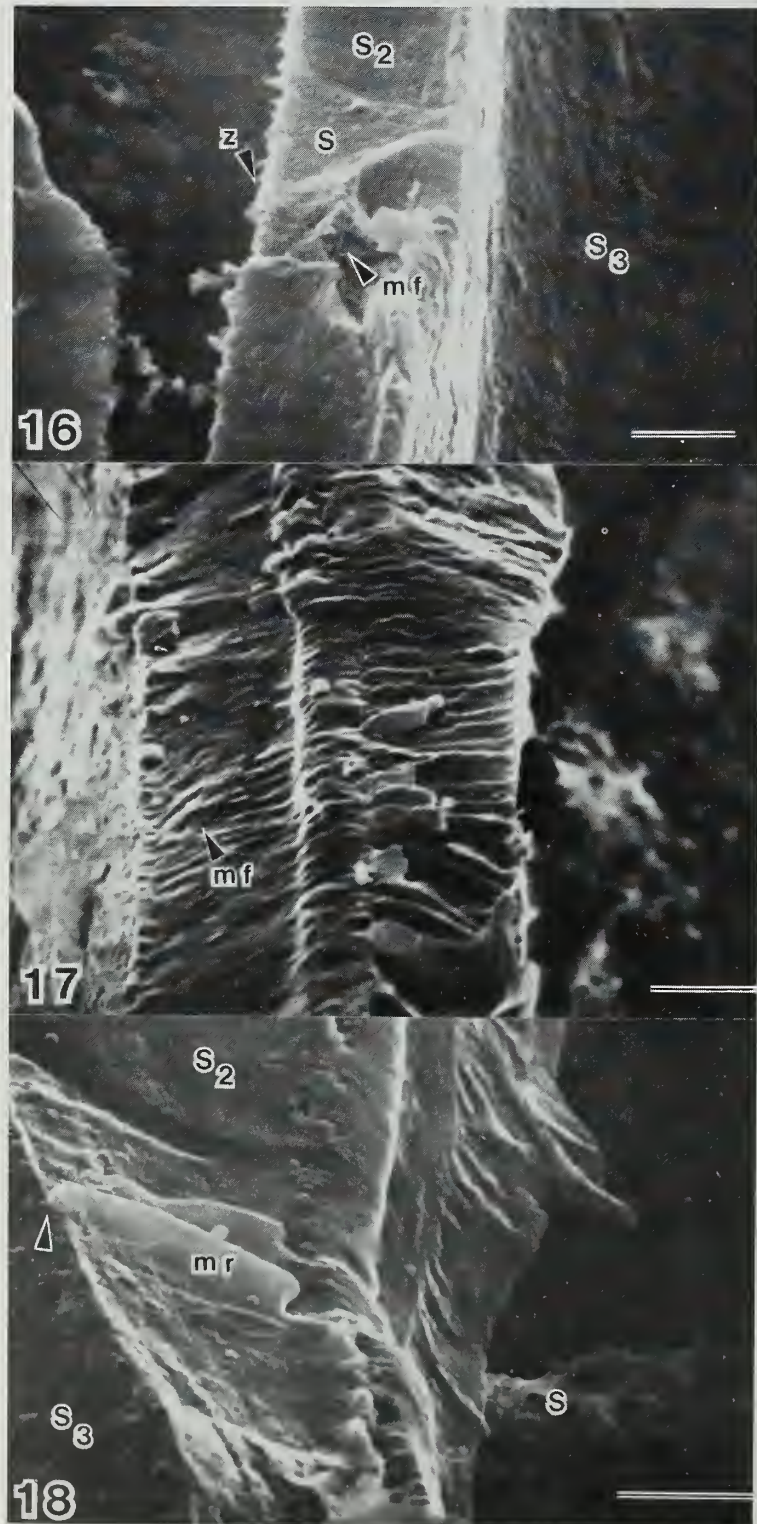




Figures 7-9. Extracellular extensions of the hyphal cell wall of P. placenta (Figs. 7-8, quenched in liquid N<sub>2</sub> and lyophilized). Fig. 7. Hyphae extending across tracheid lumen with hyphal sheath components extending from hypha to cell wall surface. Note what appears to be a hyphal track extending underneath intact hyphae to a bore hole (lower left) (x 6,000; bar = 2  $\mu$ m). Fig. 8. Increased magnification of portion of Fig. 7 depicting branched mycofibrils and vesicle-like structures (x 50,000; bar = 0.5  $\mu$ m). Fig. 9. Collapsed hyphae (h) bearing mycofibrils (mf) that are extending onto S<sub>2</sub> surface. The membranous part of the sheath appears to be absent (x 30,000; bar = 0.5  $\mu$ m; fixed in OsO<sub>4</sub> vapors and air dried).

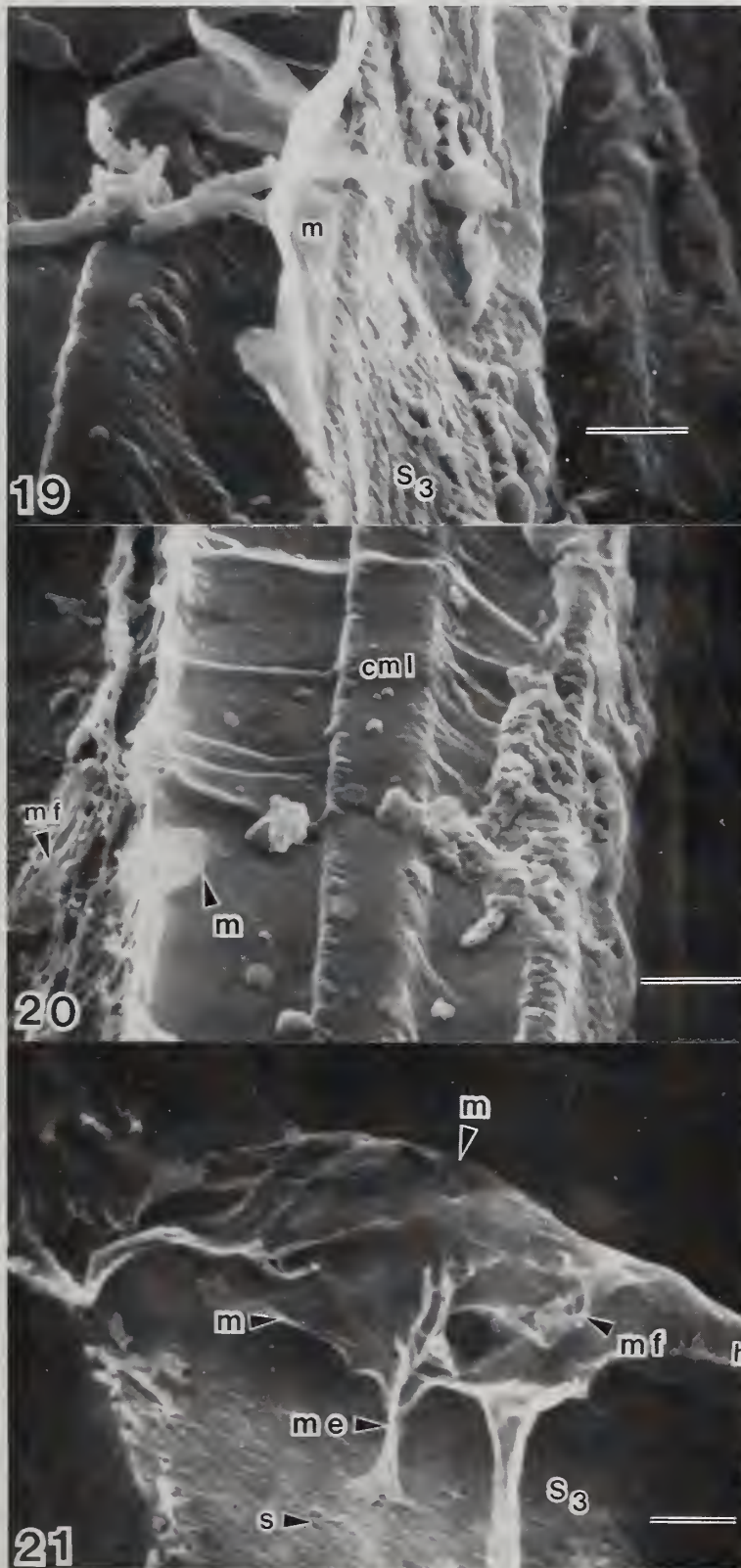


Figures 16-18. Fungal sheath components in longitudinal fracture faces of cell wall of *Pinus* decayed by *P. placenta* (quenched in liquid N<sub>2</sub> and lyophilized). Fig. 16. Penetration from modified S<sub>3</sub> into S<sub>2</sub> by mycofibrils (mf) associated with a putative membranous-like structure of the sheath (s). The zone of separation (z) is apparent at the S<sub>1</sub>-S<sub>2</sub> interface (x 15,000). Fig. 17. Topography of a longitudinally fractured cell wall. Note linear orientation of areas of penetration by mycofibrils (mf). Modified S<sub>3</sub> is apparent at left (x 15,000). Fig. 18. Sheath (s) extending through lumen space in linear apposition to membrane remnants (mr) in S<sub>2</sub> and compound middle lamella. Mycofibrils are evident at arrow (x 20,000; all bars = 1  $\mu$ m).





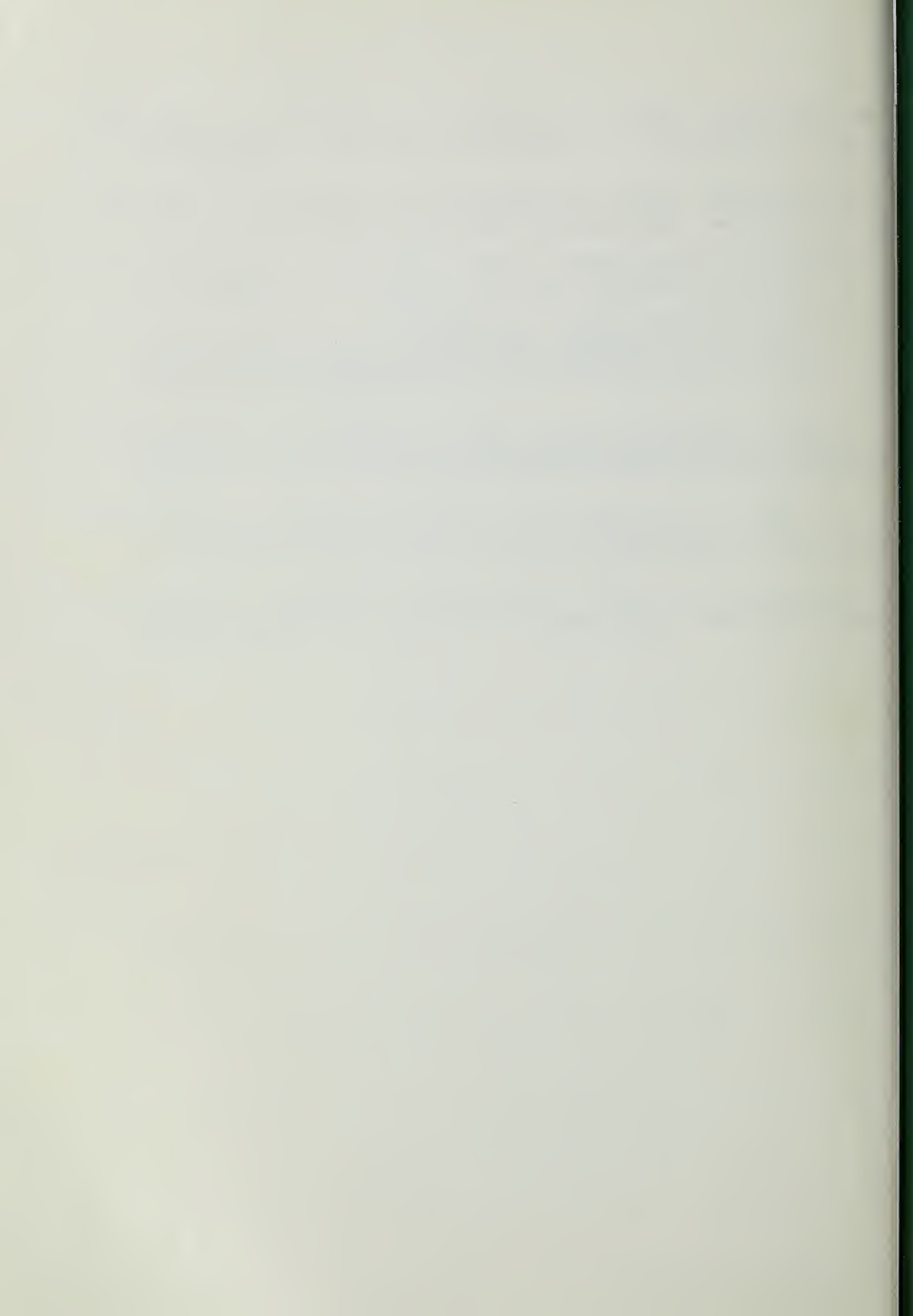
Figures 19-21. Longitudinal fracture of decayed *Pinus* sp. (quenched in liquid  $N_2$  and lyophilized). Figs. 19-20. Penetration of cell wall by mycofibrils (mf) and membranous-like structures. Note apparent tri-lamellar nature of membranous fragment attached to modified  $S_3$  (m) (x 15,000). Fig. 21. Extracellular membrane (m) extending from hyphae (h) to  $S_3$  surface. Note the morphology of the membrane extension (me) in direct contact with modified  $S_3$ . Mycofibrils (mf) can be readily seen in association with membrane (x 12,500; all bars = 1  $\mu$ m)





- [29] Palmer, J G, Murmanis, L L, and Highley, T L (1983) Visualization of hyphal sheath in wood-decay hymenomycetes. I. Brown rotters. *Mycologia* 75: 995-1004
- [30] Palmer, J G, Murmanis, L L, and Highley, T L (1984) Observations of wall-less protoplasts in white- and brown-rot fungi. *Mater Org* 19: 39-44
- [31] Parameswaran, N, and Liese, W (1982) Ultrastructural localization of wall components in wood cells. *Holz Reh- und Werkst* 40: 145-155
- [32] Ruel, K, Barnoud, F, and Eriksson, K E (1981) Micromorphological ultrastructural aspects of spruce wood degradation by wild type Sporotrichum pulverulentum and its cellulase-less mutant cell 44. *Holzforschung* 35: 157-171
- [33] Srebotnik, E, and Messner, K (1988) Spatial arrangement of lignin peroxidase in pine decayed by Phanerochaete chrysosporium and Fomitopsis pinicola. Inter Res Group On Wood Preserv Document No: IRG/WP/1343
- [34] Srebotnik, E, Messner, K, Foisner, R, and Pettersson, B (1988) Ultrastructural localization of ligninase of Phanerochaete chrysosporium by immunogold labeling. *Current Microbiol* 16: 221-227
- [35] Tsuneda, A, Koshitani, H, and Furukawa, I (1987) Micromorphological patterns of incipient wood decay by Lentinus edodes. *Rept Tottori Mycol Inst* 25: 36-48









1022299357

\* NATIONAL AGRICULTURAL LIBRARY



1022299357